AD-A119 540 AEROSPACE CORP EL SEGUNDO CA AEROPHYSICS LAB F/G 20/5
OPERATING CHARACTERISTICS OF HSURIA ANNULAR RESONATOR WITH A W---ETC(U)
JUL 82 E B TURNER, R A CHODZKO, S B MASON F04701-81-C-0082
UNCLASSIFIED TR-0082(2930-01)-6 SD-TR-82-48 NL

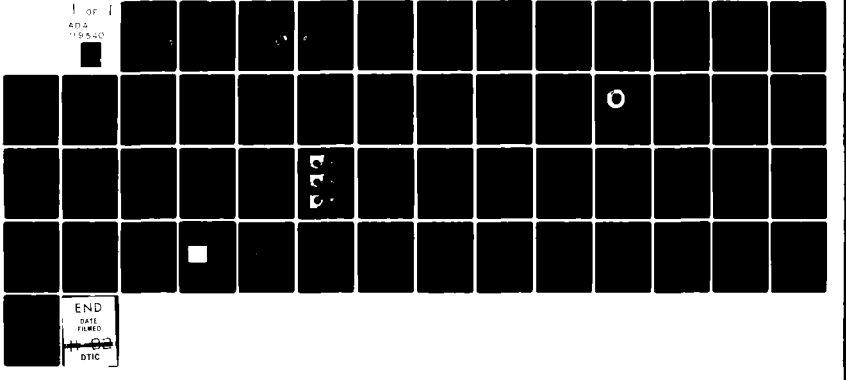

END
DATE FILMED
11-82
DTIC

REPORT SD-TR-82-48

Operating Characteristics of HSURIA Annular Resonator with a W-Axicon and a Rear Flat Cavity Mirror

E. B. TURNER, R. A. CHODZKO, and S. B. MASON
Aerophysics Laboratory
Laboratory Operations
The Aerospace Corporation
El Segundo, Calif. 90245

12 July 1982

Prepared for

SPACE DIVISION
AIR FORCE SYSTEMS COMMAND
Los Angeles Air Force Station
P.O. Box 92960, Worldway Postal Center
Los Angeles, Calif. 90009

This report was submitted by The Aerospace Corporation, El Segundo, CA 90245, under Contract No. F04701-81-C-0082 with the Space Division, Deputy for Technology, P.O. Box 92960, Worldway Postal Center, Los Angeles, CA 90009. It was reviewed and approved for The Aerospace Corporation by W. P. Thompson, Director, Aerophysics Laboratory. Lt Efren V. Fornoles, SD/YLXT was the project officer for the Mission-Oriented Investigation and Experimentation (MOIE) program.

This report has been reviewed by the Public Affairs Office (PAS) and is releasable to the National Technical Information Service (NTIS). At NTIS, it will be available to the general public, including foreign nations.

This technical report has been reviewed and is approved for publication. Publication of this report does not constitute Air Force approval of the report's findings or conclusions. It is published only for the exchange and stimulation of ideas.

Efren V. Fornoles

Efren V. Fornoles, 1st Lt, USAF
Project Officer

Jimmie H. Butler

Jimmie H. Butler, Colonel, USAF
Director of Space Systems Technology

FOR THE COMMANDER

Norman W. Lee, Jr.

Norman W. Lee, Jr., Colonel, USAF
Deputy for Technology

UNCLASSIFIED

SECURITY CLASSIFICATION OF THIS PAGE (When Data Entered)

REPORT DOCUMENTATION PAGE		READ INSTRUCTIONS BEFORE COMPLETING FORM
1. REPORT NUMBER SD-TR-82-48	2. GOVT ACCESSION NO. AD-A119540	3. RECIPIENT'S CATALOG NUMBER
4. TITLE (and Subtitle) OPERATING CHARACTERISTICS OF HSURIA ANNULAR RESONATOR WITH A W-AXICON AND A REAR FLAT CAVITY MIRROR		5. TYPE OF REPORT & PERIOD COVERED 6. PERFORMING ORG. REPORT NUMBER TR-0082(2930-01)-6
7. AUTHOR(s) Eugene B. Turner, Richard A. Chodzko, and Stephen B. Mason		8. CONTRACT OR GRANT NUMBER(s) F04701-81-C-0082
9. PERFORMING ORGANIZATION NAME AND ADDRESS The Aerospace Corporation El Segundo, Calif. 90245		10. PROGRAM ELEMENT, PROJECT, TASK AREA & WORK UNIT NUMBERS
11. CONTROLLING OFFICE NAME AND ADDRESS Space Division Air Force Systems Command Los Angeles, Calif. 90009		12. REPORT DATE 12 July 1982 13. NUMBER OF PAGES 50
14. MONITORING AGENCY NAME & ADDRESS(if different from Controlling Office)		15. SECURITY CLASS. (of this report) Unclassified 15a. DECLASSIFICATION/DOWNGRADING SCHEDULE

16. DISTRIBUTION STATEMENT (of this Report)

Approved for public release; distribution unlimited

17. DISTRIBUTION STATEMENT (of the abstract entered in Block 20, if different from Report)

18. SUPPLEMENTARY NOTES

19. KEY WORDS (Continue on reverse side if necessary and identify by block number)

Annular Gain Geometry
Optical Misalignment Sensitivity
Effect of Struts
Effect of W-Axicon Tip Obscuration
Half-Symmetric Unstable Resonator with Internal Axicon (HSURIA)
Optical Laser Resonator

20. ABSTRACT (Continue on reverse side if necessary and identify by block number)

In this report are presented the results of tests performed on the half-symmetric unstable resonator with an internal axicon (HSURIA) using a large-diameter, closed-cycle CO_2 laser facility. The HSURIA used for these tests consisted of a linear W-axicon, a convex spherical feedback mirror, and a flat rear cavity mirror. This resonator produced a linearly polarized $\ell = 0$ mode of good beam quality. Tests were designed to investigate several critical issues related to the use of the HSURIA with a cylindrical chemical laser, ...

DD FORM 1473 (FACSIMILE)

UNCLASSIFIED

SECURITY CLASSIFICATION OF THIS PAGE (When Data Entered)

19. KEY WORDS (Continued)

20. ABSTRACT (Continued)

namely, the misalignment sensitivity of the elements, optical effects of support struts, and the feasibility of reducing the high flux on the W-axicon tip by obscuration of the tip. Tests were performed for a variety of resonator configurations with different parameters. The beam quality was rapidly degraded by small angular misalignments of the rear flat but was scarcely affected by much larger misalignments of the feedback mirror. The insertion of strut masks resulted in an unexpectedly large power loss. Analysis indicates that these losses are caused by diffraction effects combined with partial saturation of the medium. A small effective obscuration o. the W-axicon tip had little effect on the mode or beam quality, but obscuration diameters with a Fresnel number approaching unity (referred to as the compacted leg length) caused a loss of mode control and a large degradation in beam quality. Finally, a pair of reflection polarizers inserted in the compact leg effectively controlled the direction of polarization that had fluctuated in a random direction.

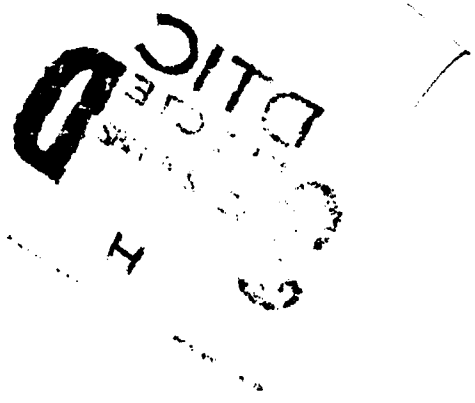

ACKNOWLEDGMENTS

The authors thank M. E. Gerard of the Aerophysics Laboratory in the performance of the experiments. We are grateful for the support of the Air Force Weapons Laboratory and Lt. Col. Plummer, Contracting Officer.

We also thank Dr. J. W. Ellinwood for the diffraction calculations, and helpful discussions from Dr. H. Mirels of the Aerophysics Laboratory.

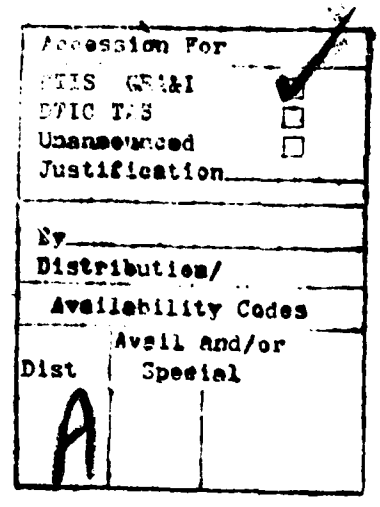

CONTENTS

FIGURES

TABLES

I. *INTRODUCTION*

In this report are presented the results of tests performed on a half-symmetric unstable resonator with an internal axicon (HSURIA) using a large-diameter, closed-cycle CO_2 laser facility.[1] In a previous study, it was determined that HSURIAs with conical rear cavity mirrors used to reduce misalignment sensitivity produced linear polarization in the azimuthal direction in the near field that resulted in a donut-shaped $\ell = 1$ mode in the far field.[2] It was possible, however, to produce a uniformly linearly polarized $\ell = 0$ mode by using a flat rear mirror instead of a conical mirror although the flat mirror was quite sensitive to misalignment.

The tests described in this report are confined to the annular HSURIA with a W-axicon beam compactor and a flat rear mirror. These tests were designed to investigate several critical issues related to the use of the HSURIA with a cylindrical chemical laser. The first issue is the sensitivity to misalignment of the rear flat cavity mirror and the convex feedback mirror. The second issue is the power loss and beam quality degradation caused by the use of struts to support the cylindrical laser gain generator inside the optical resonator cavity. The final issue is the feasibility of reducing the heat flux on the W-axicon tip by an obscuration of part of the laser beam that would be incident on the tip. The obscuration diameter should be sufficiently large to reduce the laser radiation flux on the tip but not large enough to degrade beam quality. The experimental tests described in this report provide quantitative answers to these critical issues. In addition, measurements were made on the polarization of the laser beam, and an intracavity reflection polarizer was successfully used to control the direction of polarization.

In the next section, the resonator configurations used for these tests are described, parameters are calculated, and the performance of each resonator is given. Measurements of laser beam quality degradation caused by the misalignment of the rear flat or the convex feedback mirror are presented in Section III. Data on power loss and beam quality degradation caused by struts are presented in Section IV, measurements on the beam quality degradation

resulting from W-axicon tip obscuration and the thermocouple measurements of the radiation field near the W-axicon tip are presented in Section V, and polarization measurements and tests of the intercavity polarizer are described in Section VI.

II. RESONATOR CONFIGURATIONS AND LASER OUTPUT CHARACTERISTICS

The gain medium of the closed-cycle CO_2 laser facility is 94 cm long; it has a fairly uniform zero power gain of 1.2 to 1.3/m over an annular region of 10 to 18.4 cm diameter that is used by the HSURIA. A rapidly flowing gas mixture of 1:1:4 of CO_2:N_2:N_2:He at a pressure of 3.5 Torr is pulsed at a rate of 10 to 15 pulse/sec with a 5.5-amp square current pulse of about 1.2 msec duration. The resulting laser output pulses have a duration of about 1.0 msec, and the average output laser power ranges from 7.5 to 9 W at 10 pulse/sec for all the resonators described in this report.

A diagram of a typical HSURIA resonator used in these tests is shown in Fig. 1. The length of the annular leg, L_A, was fixed. It is the sum of the distances from the rear flat to the turning flat axis, namely, 1.92 m and the distance between the W-axicon tip and the turning flat, 0.19 m. Thus, L_A = 2.11 m. There is a transition distance, L_T, of 0.09 m from the tip of the W-axicon to the outer cone. The distance from the convex feedback mirror to the W-axicon tip is L_C, the compacted length, and the sum of L_A, L_T, and L_C is the total cavity length, L. The radius of curvature of the spherical convex feedback mirror is R.

The magnification of a half-symmetric unstable resonator is given by

$$M = \frac{[1 + (R/L)]^{1/2} + 1}{[1 + (R/L)]^{1/2} - 1} \qquad (1)$$

where R is taken as positive. The actual ratio of the outer diameter of the laser output beam to the inner obscured diameter is slightly less, however, because the scraper is located a distance s from the convex mirror. This ratio, which will be designated as M_S, is given by

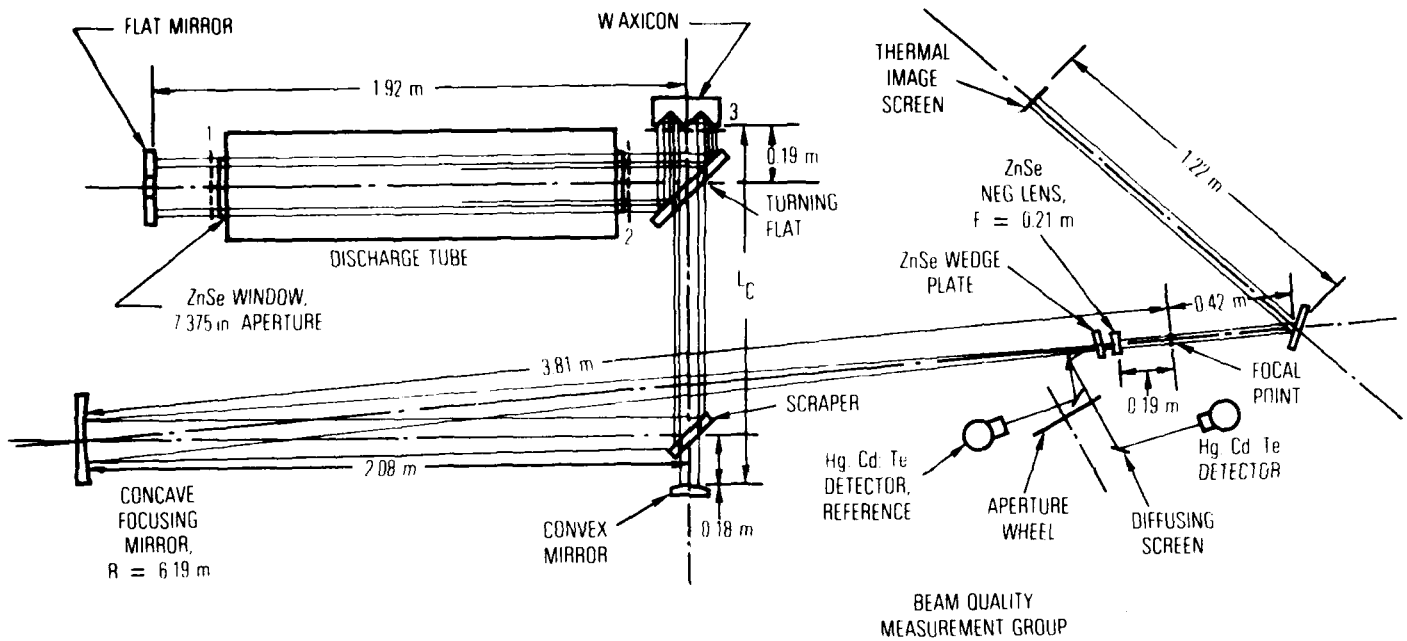

Fig. 1. Diagram of a Typical HSURIA Resonator Used in Tests. Positions 1, 2, and 3 are locations of strut masks, and L_C is the length of the compacted leg.

$$M_S = \frac{[1 + (R/L)]^{1/2} + 1 - S/L}{[1 + (R/L)]^{1/2} - 1 + S/L} \tag{2}$$

and it is used for the calculation of the theoretical far-field pattern. The value of M_S for the three convex mirror radii used in these tests is plotted versus the cavity length in Fig. 2.

The equivalent Fresnel number of a half-symmetric unstable resonator is given by the formula,

$$N_{eq} = \frac{a^2}{2\lambda L}\left(\frac{M^2 - 1}{2M}\right) \tag{3}$$

when the laser beam exits around the outside of the convex mirror of radius a. When a scraper, or outcoupling mirror, is used, however, the radius, a, is the projection of the scraper hole radius on the convex mirror, namely,

$$a = \frac{[1 + (R/L)]^{1/2} - 1}{[1 + (R/L)]^{1/2} - 1 + S/L}\, a_0 \tag{4}$$

where $2a_0$ is the diameter of the hole in the scraper mirror. Salvi[3] has shown that a further correction should be applied to obtain the corrected N_{eqc} for outcoupling with a scraper mirror.

$$\frac{1}{N_{eqc}} = \frac{1}{N_{eq}} - \frac{1}{N_d} \tag{5}$$

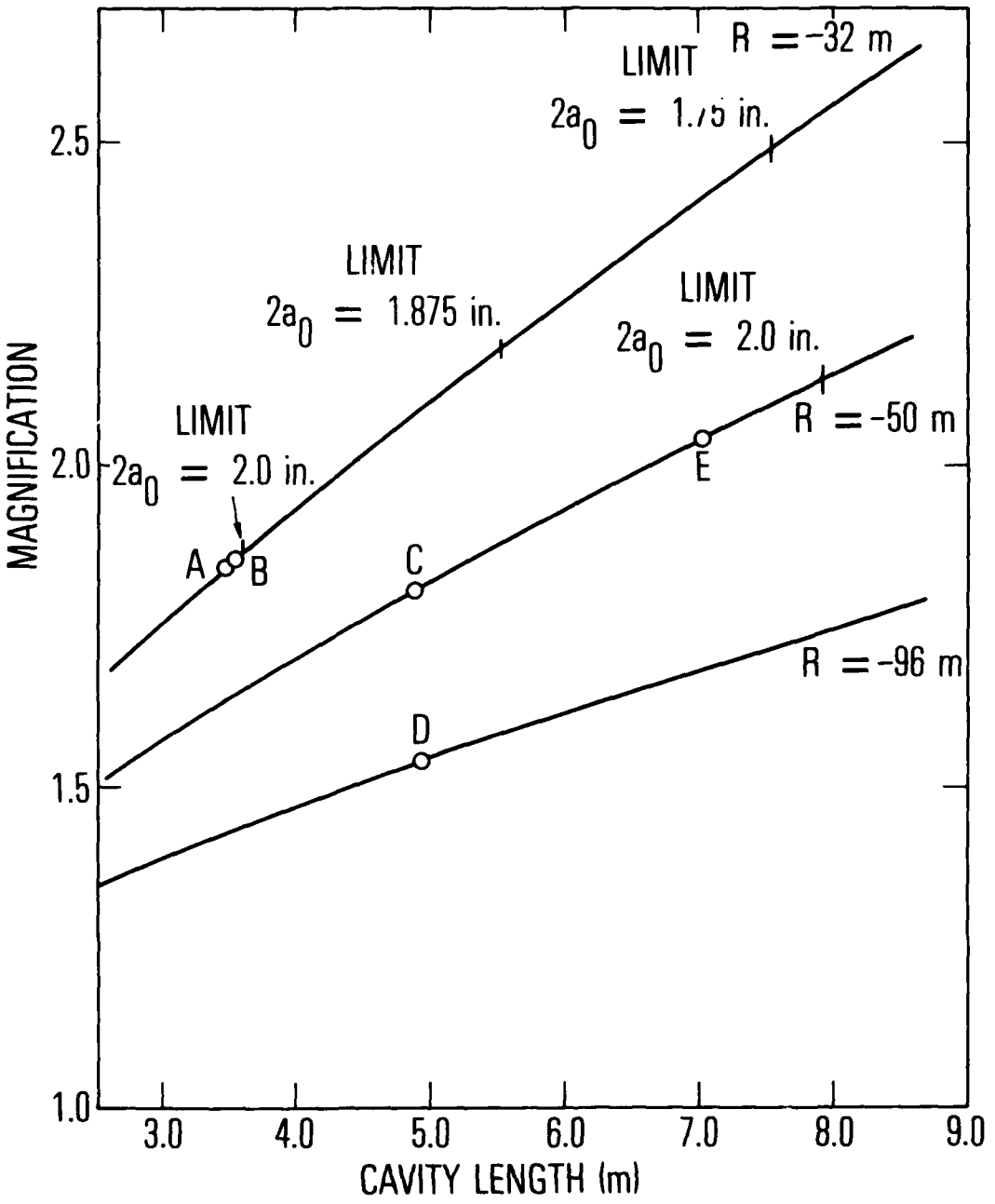

Fig. 2. Magnification vs Cavity Length for Several Convex Mirror Radii. The limit values indicated on the curves are the values for which the size of the near-field pattern, $2\sqrt{2}\, a_0 M$, exceeds the width of the scraper mirror of 15 cm.

where

$$N_d = \frac{aa_0}{\lambda S}$$

Curves of this corrected equivalent Fresnel number are plotted versus the cavity length in Fig. 3 for various combinations of convex mirror radii and scraper hole diameters that were used for these tests.

Parameters of various resonator configurations used in these tests are shown by locations designated by the letters A through E on these curves and on the curves of M_S versus L of Fig. 2.

Most of the resonator parameters were originally selected to produce half-integral equivalent Fresnel numbers. With Salvi's correction, however, the N_{eqc} was slightly greater. Most tests were performed with resonators A and B, which are almost identical. Experiments were conducted with longer compacted leg lengths, C and E, to explore the effect on strut losses and tip obscuration, and some tests were run at low values of magnification, D, to increase the saturation of the gain medium and determine the effect on strut loss. A summary of the resonator parameters used in these experiments is given in Table 1.

The beam quality, n^2, as used in this report, is defined as the ratio of the theoretical fraction of energy within the diameter of the far-field central lobe to the actual fraction of energy within this diameter. The theoretical fraction of energy within a given diameter is determined by integrating the far-field intensity distribution, which is the Fraunhofer diffraction pattern from a uniformly illuminated annular aperture, namely,

$$W(y) = \frac{1}{2(1 - \varepsilon^2)} \int_0^y \left[\frac{2J_1(y')}{y'} - \varepsilon^2 \frac{2J_1(\varepsilon y')}{\varepsilon y'}\right]^2 y' dy' \qquad (6)$$

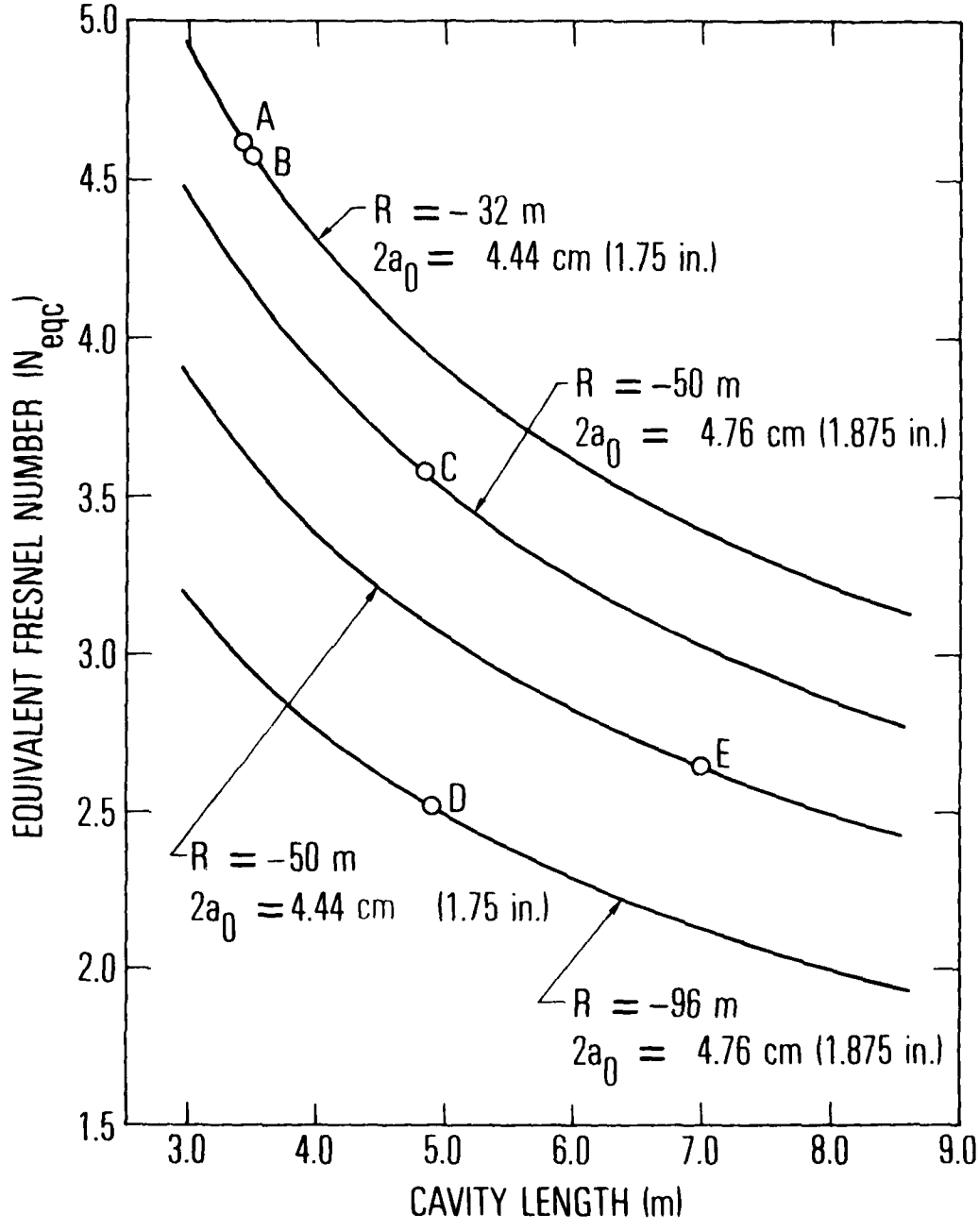

Fig. 3. Equivalent Fresnel Number vs Cavity Length for Several Combinations of Convex Mirror Radii and Scraper Hole Diameter

Table 1. Summary of Resonator Parameters

Resonator Designation	L_C	L (m)	R (m)	M	M_S	$2a_0$ (in.)	N_{eq}
A	1.25	3.45	32	1.91	1.84	1.75	4.62
B	1.30	3.51	32	1.92	1.85	1.75	4.60
C	2.66	4.86	50	1.85	1.80	1.875	3.58
D	2.72	4.92	96	1.57	1.54	1.875	2.52
E	4.81	7.01	50	2.08	2.04	1.75	2.63

This integral is normalized to unity for $y \to \infty$. $J_1(y)$ is the Bessel's function, and ε is the ratio of the inner to the outer diameter of the annulus.

$$\varepsilon = \frac{1}{M_S}$$

The argument y in the Fraunhofer diffraction pattern is equal to $kr\alpha$, where k is the wavenumber, $2\pi/\lambda$; r is the outer radius of the annular aperture; and α is the angle of the far-field radius observed from the aperture location.

Theoretical curves for several values of resonator magnification used in these experiments are shown in Fig. 4, along with a curve for an unobscured circular aperture ($M = \infty$) that is shown for comparison. The fraction of power in the central lobe varies from 32% for $M_S = 1.54$ to 49% for $M_S = 2.04$.

The experimental beam quality curve, i.e., a curve of the fraction of power within a given diameter in the far field, was obtained by focusing a fraction of the laser beam reflected from a beam splitter onto an aperture plate with hole sizes from 0.010 to 0.060 in. diameter and with one large hole of 0.500 in. diameter, which transmitted nearly 100% of the beam. The aperture plate was rotated with a stepper motor to put the various apertures at the focus of the beam. The energy transmitted through the apertures was measured with a laser power meter or with a Hg:Cd:Te detector using a scattering plate. The diameter of the aperture is related to the argument, y, by the formula

$$d = \frac{2\lambda F}{\pi D} y \qquad (7)$$

obtained from the definition of y given previously, where D is the outer diameter of the laser beam on the concave focusing mirror, F is the distance from this mirror to the focus, and λ is the wavelength of the laser radiation. The

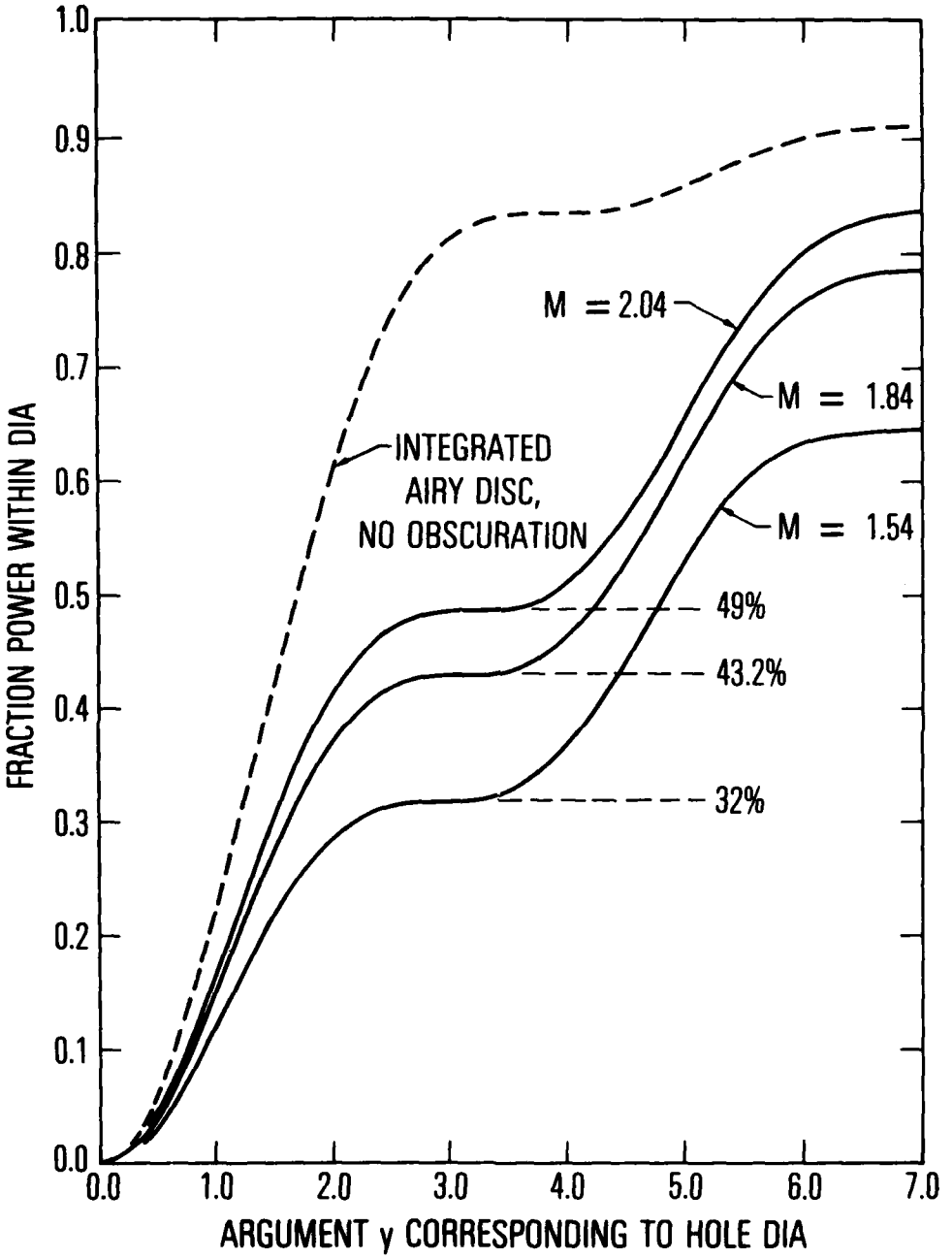

Fig. 4. Integrated Power within a Given Diameter in the Far Field

first null in the integrand of Eq. (6) occurs at a value of the argument that will be designated as y_0. This, of course, varies with the value of ϵ or M_s, as indicated in Table 2. The first null in the theoretical far-field pattern should then occur at a diameter d_0 that corresponds to the value of the argument y_0 according to Eq. (7). The central lobe should then be contained within the diameter d_0, which is often called the diameter of the bucket, and the laser beam power within this diameter is called the power in the bucket, which is designated by P_0. The ratio of P_0 to the total power P_∞ is given in Table 2.

A typical experimental beam quality curve is shown in Fig. 5 for resonator A. The bucket diameter for this case is 0.033 in., and the measured fraction of energy transmitted at this diameter is 34%. The theoretical value is 43.2%, so the beam quality n^2 is 1.27. A summary of the measured beam quality data for the five resonator configurations with no misalignment, struts, or other obscurations in the resonator cavity is given in Table 2. The beam quality n^2 is slightly larger than unity for all the resonators tested. The principal reason for this degradation is that aberrations occur in the W-axicon that are clearly shown in the interferograms of the flat mirror-W-axicon combination.[2] The beam quality for all resonator configurations tested was sufficient to determine the degradation caused by mirror misalignment, struts, W-axicon tip obscuration, etc. Typical photographs of the near- and far-field patterns on a thermal image screen are shown in Fig. 6.

Table 2. Beam Quality Data

Resonator Designation	$\frac{d\ (in.)}{y}$	First Null		$\left(\frac{P_0}{P_\infty}\right)_{theor}$	$\left(\frac{P_0}{P_\infty}\right)_{exp}$	Beam Quality (n^2)	M_S
		y_0	d_0 (in.)				
A	0.01081	3.08	0.0333	0.432	0.34	1.27	1.84
B	0.01097	3.085	0.0339	0.435	0.34	1.28	1.85
C	0.00960	3.06	0.0294	0.419	0.30	1.40	1.80
D	0.01081	2.90	0.03135	0.320	0.28	1.14	1.54
E	0.00856	3.16	0.02706	0.490	0.425	1.15	2.04

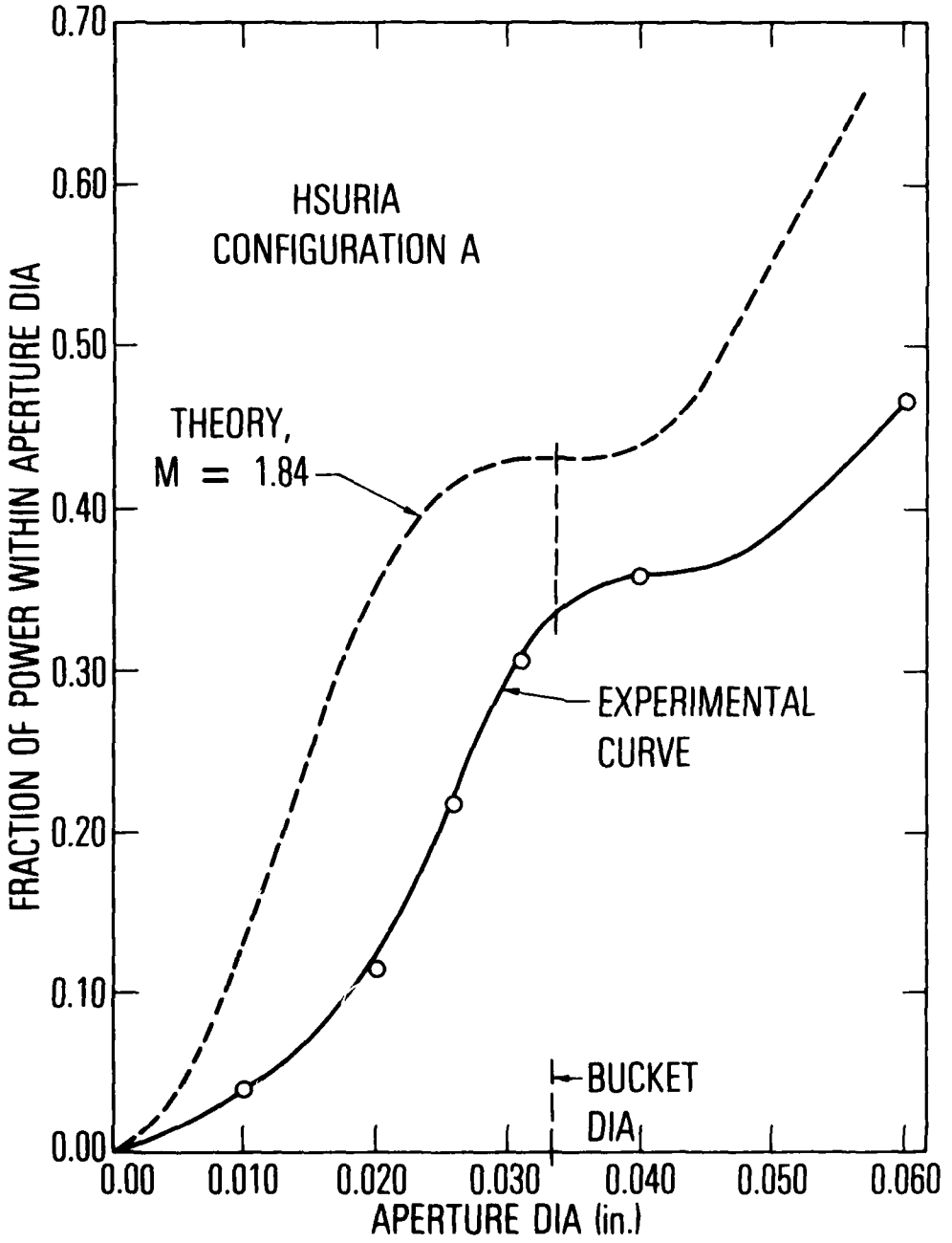

Fig. 5. Experimental Beam Quality Curve for Resonator A

Fig. 6. Typical Near- and Far-Field Laser Beam Intensity Patterns

III. MISALIGNMENT SENSITIVITY OF CAVITY MIRRORS

The primary disadvantage of the HSURIA resonator with a rear flat cavity mirror is the sensitivity of the laser beam quality to misalignment of this mirror. This was reported previously for the resonator configuration A.[2] The beam quality degradation caused by misalignment of the rear flat mirror was measured for a couple of additional resonator configurations, namely C and D, and the results were similar to those reported for A.[2] These results, given in Fig. 7, show that the fraction of power in the central lobe suffers a significant decrease for a mirror misalignment of ±5 μrad. Indeed, it was necessary to periodically tweak the rear flat gimbal adjustment to maintain the best beam quality.

The laser beam quality is, on the other hand, relatively insensitive to misalignment of the convex feedback mirror. Figure 8 shows the beam quality degradation for HSURIA configurations C and D as a function of the misalignment angle of the convex mirror. The beam quality remains relatively good for misalignments of up to 200 μrad, but degrades rapidly for greater misalignment angles. Near- and far-field beam patterns with misaligned resonator mirrors of A were provided in Ref. 2. The convex mirror is, therefore, a factor of 20 less sensitive to misalignment than the rear flat mirror for all resonator configurations tested.

An angular misalignment α of a convex spherical resonator mirror of radius R (in a half-symmetric unstable resonator with a flat rear mirror) will move the optic axis laterally by a distance αR, because as a condition for resonance, the optic axis must be perpendicular to the surfaces of both the convex and the flat mirrors. This causes the outer diameter of the laser output beam to shift toward the fixed inner obscuration diameter, and the near-field pattern becomes asymmetric. Krupke and Sooy[4] studied the effects of misalignment in a confocal, unstable resonator. They observed that as long as the optic axis (and a region of diameter $\sqrt{\lambda L}$ around it) lay within the boundaries of both mirrors, the mode will be essentially a lowest order geometric mode. Using this criterion for our HSURIA resonators, which we

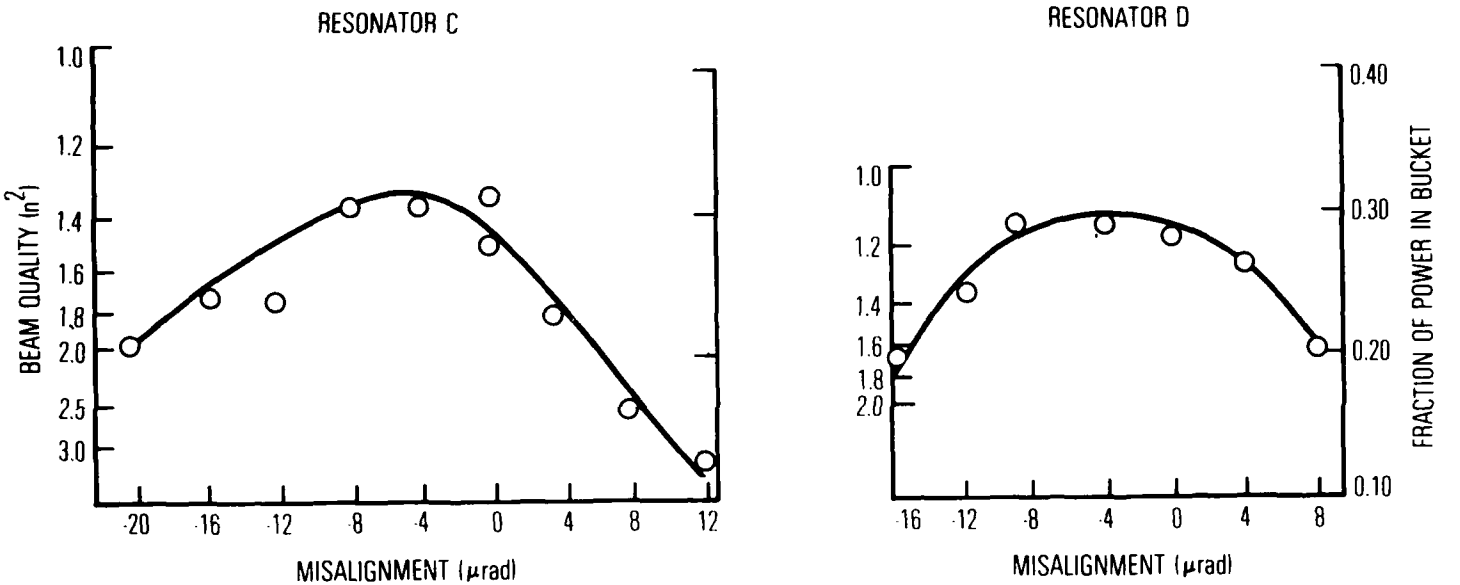

Fig. 7. Misalignment Sensitivity of Rear Flat Mirror for Two HSURIA Configurations

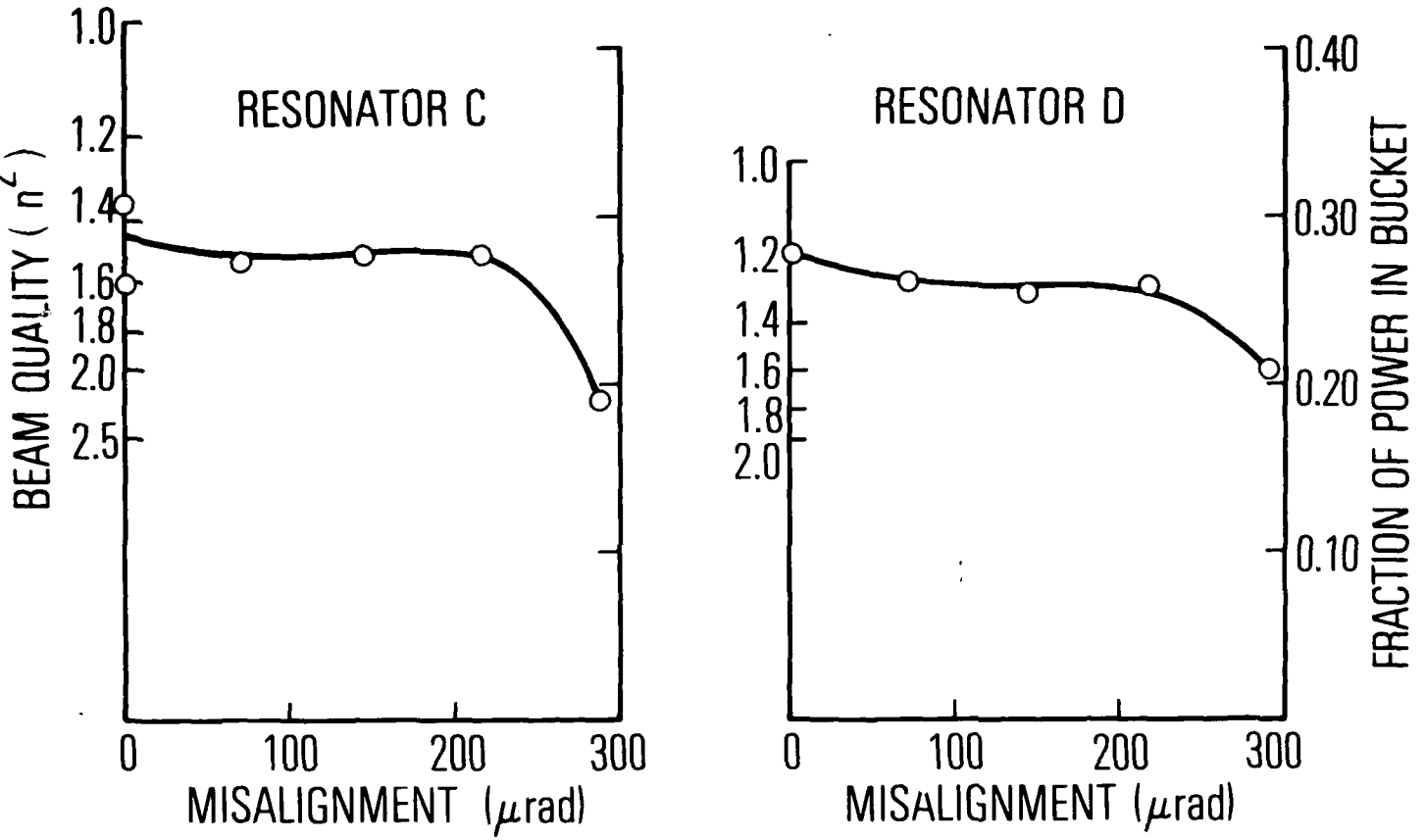

Fig. 8. Misalignment Sensitivity of Convex Feedback Mirror for Two HSURIA Configurations

approximate as a half-symmetric unstable resonator, one would not expect degradation as long as

$$\alpha R < (a - \frac{\sqrt{\lambda L}}{2})$$

For typical values of a = 0.02 m, R = 50 m, and L = 5 m

$$\alpha R < 0.016 \text{ m or } \alpha < 320 \text{ } \mu\text{rad}$$

This is somewhat larger than the measured value of 200 μrad.

IV. POWER LOSS AND BEAM DEGRADATION CAUSED BY STRUTS

In a cylindrical laser, the gain generator must be supported within the resonator cavity by struts, and it is important to determine the effect of these struts on the laser output power and beam quality. The struts were simulated by masks that are shown in Fig. 9. The strut masks could be mounted on the window frames of the discharge tube or in a frame directly in front of the W-axicon (positions 1, 2, and 3 in Fig. 2). The masks usually consisted of six struts of either 2-1/2 or 5 deg, although masks with only three struts were also tested. A summary of the results is presented in Table 3. Four resonator configurations were used to obtain data over a range of magnifications and compacted leg lengths. The degradation of laser output power caused by the struts was much greater than the fraction of geometric obscuration. For a strut mask consisting of six 2-1/2-deg struts, the geometric obscuration is only 4.17%, but the power loss was about 25% or six times the geometric value when this strut mask was placed in front of the W-axicon.

In a half-symmetric unstable resonator, a beam must pass the struts several times as it expands from a small diffraction-limited core on the axis to a diameter that is finally reflected out of the resonator by the scraper mirror. The effect of diffraction on the power caused by struts can, therefore, be modeled approximately as a beam that traverses the struts ten times (i.e., five roundtrips for a typical unstable cavity). This analysis, developed by J. W. Ellinwood, is discussed in the Appendix, and the result indicates a power loss of about 2.5 times the geometric value for 2-1/2-deg struts, which is less than the observed value of six. The additional loss is believed to be caused by a lack of gain saturation of the CO_2 gain cell. Strut blockage in the annular leg of the HSURIA can be considered as an approximate effective reflection loss resulting from diffractive mixing in the compact leg.[6] This reduced reflectivity will decrease the threshold gain, and reduce the power extraction as discussed in the Appendix.

In the present experiments, the zero power gain was less than twice the threshold gain; therefore, the CO_2 gain medium was relatively unsaturated.

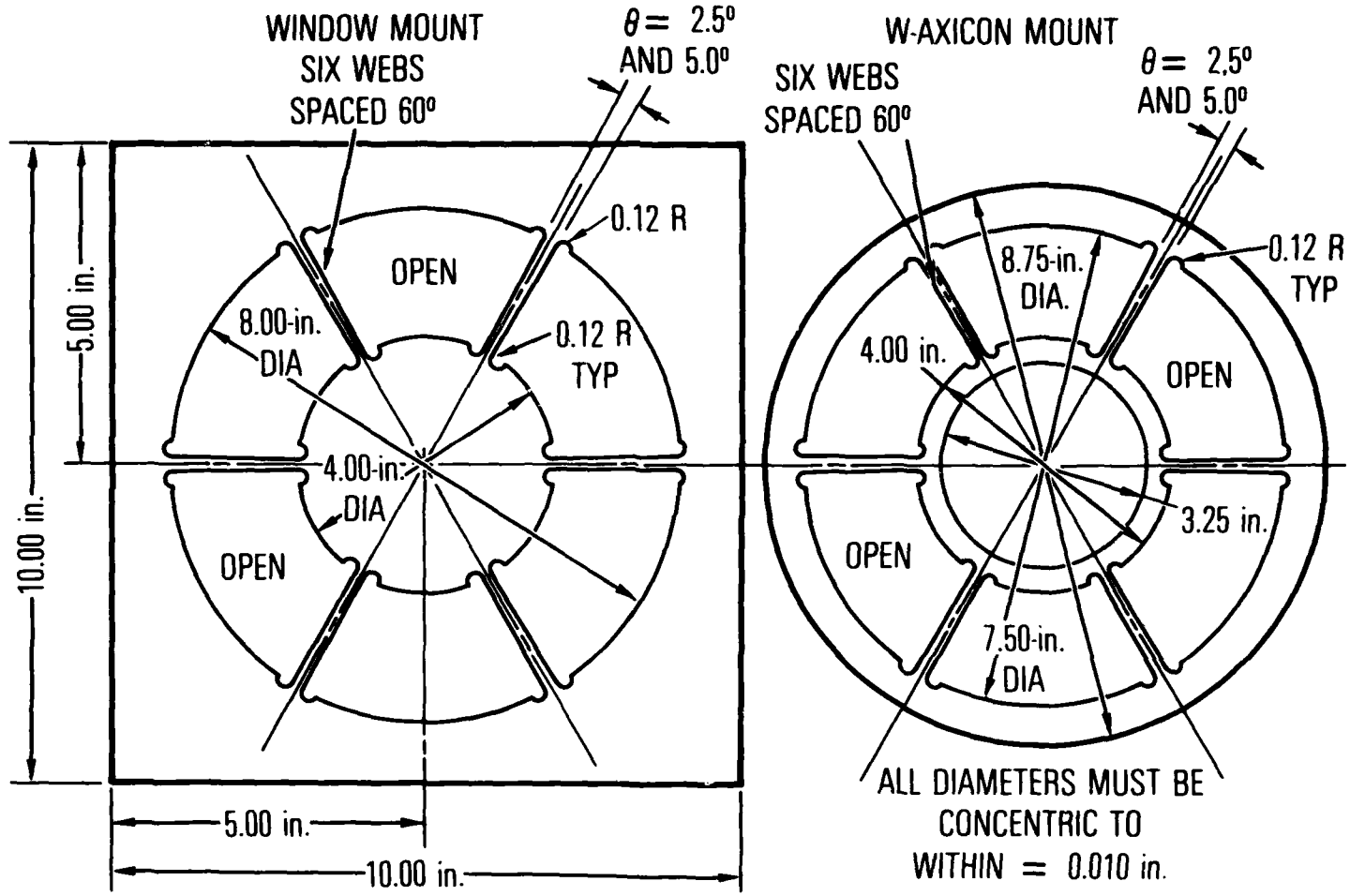

Fig. 9. Strut Masks

Table 3. Summary of Experimental Data on Struts

HSURIA Configuration	Strut Mask	Strut Position[a]	Power Loss (%)	Power Loss Geometric Loss	Beam Quality (n^2)
B	None				1.27
L = 3.51 m, M_S = 1.85	Six 2-1/2 deg	1	14.3	3.43	1.37
	Six 2-1/2 deg	2	25	6.00	1.44
	Six 5 deg	1	20	2.40	1.49
	Six 5 deg	2	27.3	3.27	1.49
	Six 2-1/2 deg	3	26.3	6.30	1.54
	Six 2-1/2 deg	1 and 3	26	6.24	1.54
	Six 5 deg	3	30	3.60	1.70
C	None				1.32
L = 4.86 m, M_S = 1.80	Six 0.006-in. dia	2	0		1.26
	Six 0.020-in. dia	2	0		1.28
	Six 0.051-in. dia	2	13.3	8.11	1.31
	Six 2-1/2 deg	1 and 3			1.58
	Six 2-1/2 deg	2	25	6.00	
	Three 2-1/2 deg	2	8.3	4.00	
	Six 5 deg	2	31	3.72	
	Three 5 deg	2	13.8	3.31	
D	None				1.14
L = 4.92 m, M_S = 1.54	Six 2-1/2 deg	3	25.7	6.16	1.28
	Six 5 deg	3	28	3.36	1.36
	Six 2-1/2 deg	1	19.2	4.60	1.28
	Six 2-1/2 deg	1 and 3	25	6.00	1.45
	Six 5 deg	3	26.2	3.14	
	Six 5 deg	1 and 3	30.5	3.66	1.68
E	None				1.19
L = 7.01 m, M_S = 2.04	Six 2-1/2 deg	3	25	6.00	1.35
	Six 5 deg	3	28	3.36	

[a] 1-Far Window, 2-Near Window, 3-W-Axicon } See Fig. 1

For unsaturated conditions, a small change in reflectivity, which is equivalent to strut loss, will produce a large change in output power. Thus, the observed output power loss, resulting from six 2-1/2-deg struts of six times the geometric value, is caused by lack of gain saturation and diffraction loss factors. A complete analysis, taking into account both diffraction effects within the resonator and gain saturation, was performed by Seminov.[6] This detailed analysis correctly predicted our power loss measurements of 25 and 30% for six 2-1/2- and 5-deg struts (at the W-axicon position), respectively.

When the mask with six struts was replaced by one with three struts, the output power loss was decreased by approximately a factor of two as expected. The differences shown in Table 3 are more than half, but the accuracy of these loss measurements was only ±4% because of output power fluctuations. Note in Table 3 that a second strut mask located at position 1 caused very little additional power loss when a strut mask was already located at position 3, provided that the two masks were properly aligned.

A photograph of the near-field patterns for HSURIA configuration E is shown in Fig. 10. The calculated intensity distribution, caused by diffraction for a single 2-1/2-deg strut after one and ten passes neglecting gain saturation effects, is shown in the Appendix in Fig. A-1. The calculated angular width of the first maxima is about ten times the geometric width. This is in reasonable agreement with the measured width of the first maxima of about eight times the geometric strut width (Fig. 10). The near-field intensity distribution obtained with a strut mask is a complex diffraction pattern that could degrade the beam quality. The beam quality degradation caused by struts was also calculated by Seminov[7] and the results are in reasonable agreement with our measurements. The use of six 2-1/2-deg struts in two places causes the beam quality index n^2 to increase from about 1.3 to 1.55 for HSURIA configurations B and C, from 1.14 to 1.45 for configuration D, and from 1.19 to 1.35 for configuration E. The use of 5-deg struts causes a greater deterioration of beam quality. The characteristics of this beam degradation are shown by the beam quality curves in Figs. 11(a) and 11(b).

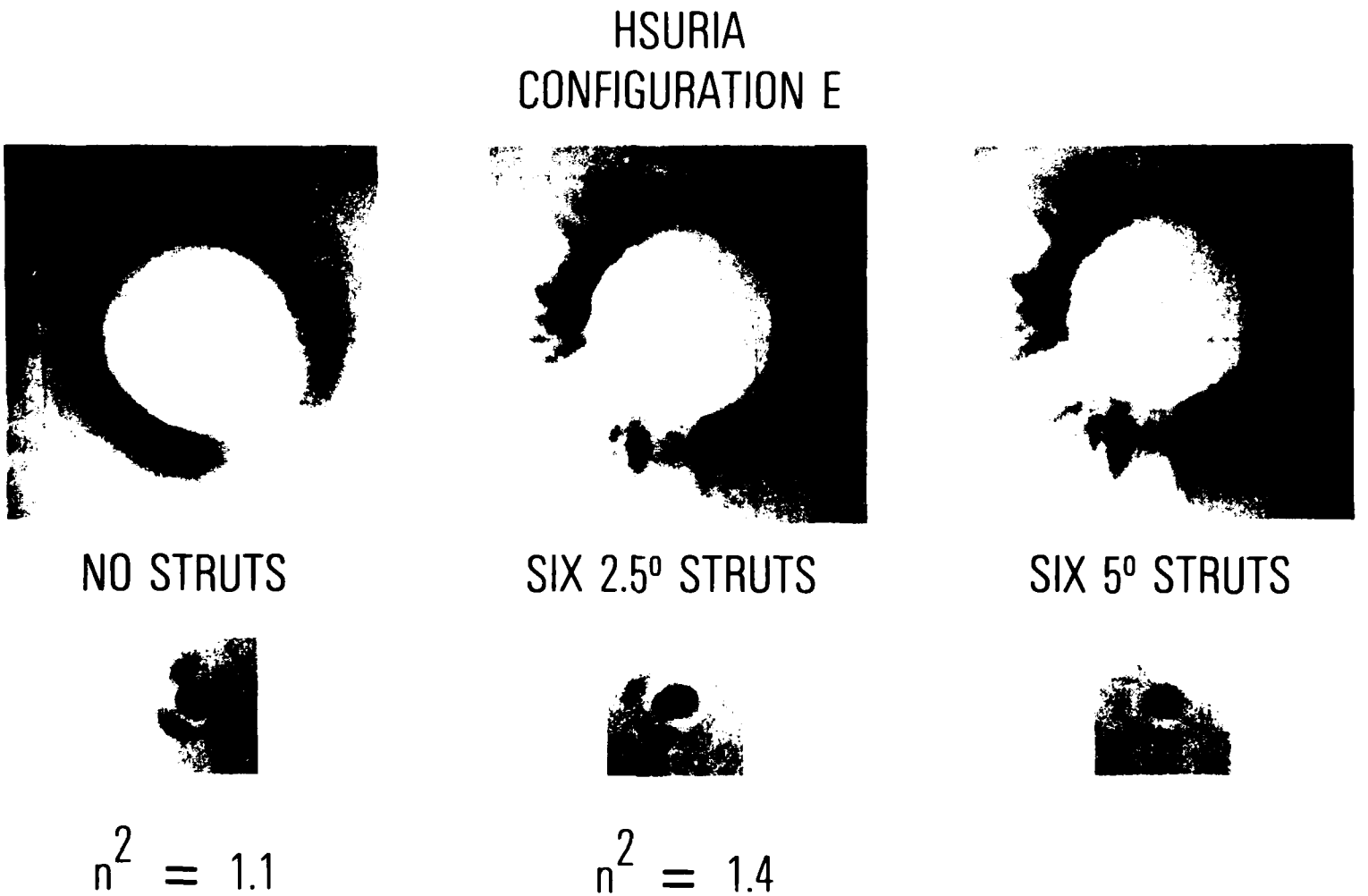

Fig. 10. Near- and Far-Field Laser Beam Intensity Distribution with and without Struts

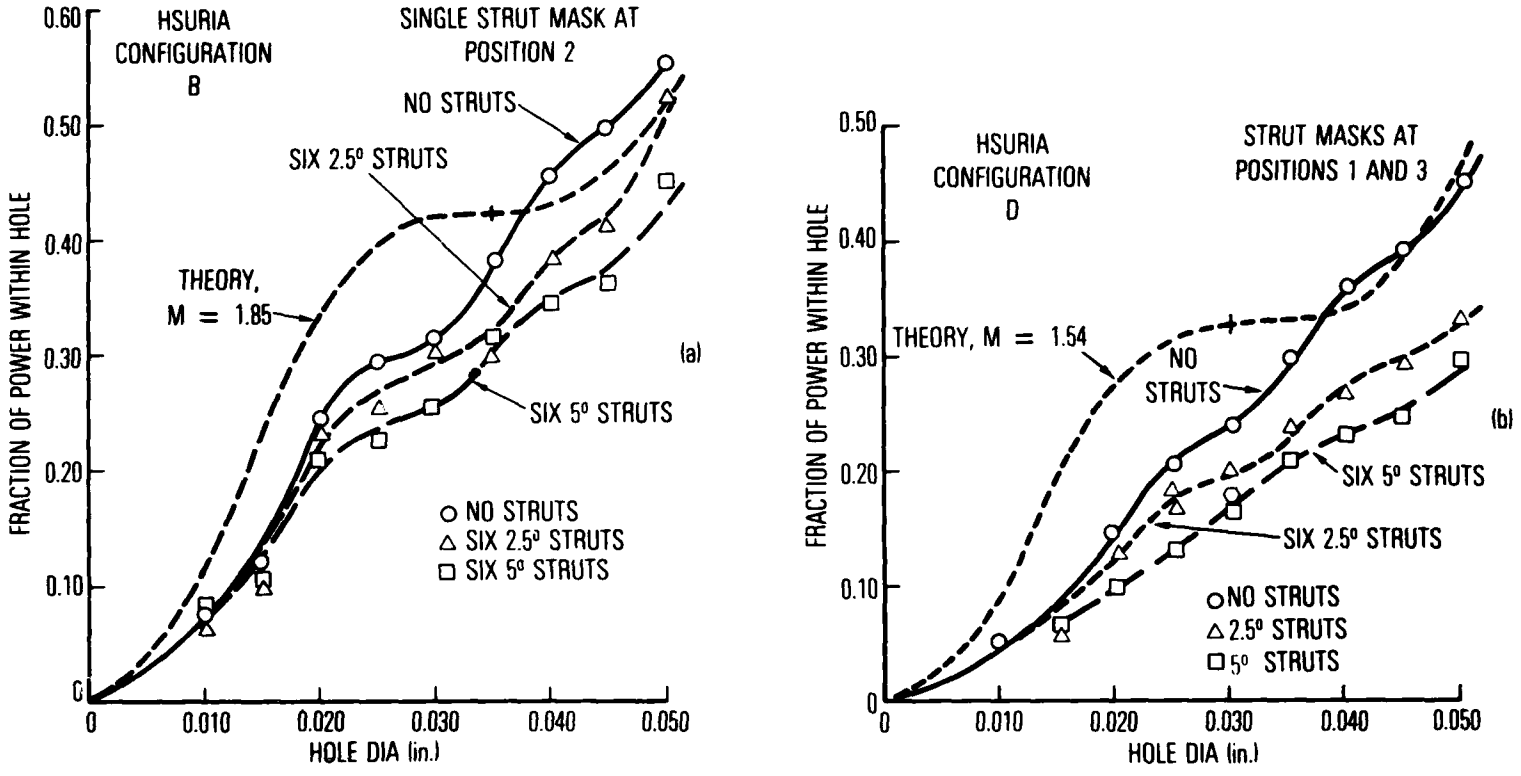

Fig. 11. Experimental Data on Beam Quality Degradation by Struts

An experiment was performed with HSURIA configuration C to determine the minimum strut size that causes a loss of power. No power loss was observed for wire strut diameters of 0.006 and 0.020 in., but a wire diameter of 0.051 in. caused a significant power loss of approximately eight times the geometric obscuration. For the wider, 5-deg struts, however, the power loss was about 3.5 times geometric. Thus, as might be expected for the wider struts, the relative effects of diffraction are reduced. The degrading effects of the struts should decrease with shorter wavelength, since the diffraction patterns from each of the struts will become smaller.

V. OBSCURATION OF THE W-AXICON TIP

In a HSURIA used with a high-power cylindrical laser, there would be a high-flux density on the tip of the W-axicon or reflaxicon. It has been proposed that this flux density could be reduced by a partial obscuration of the beam at the optic axis. This could be done by a circular aperture of a diameter slightly smaller (for a W-axicon) than the diameter of the optic axis. This obscuration, however, will also degrade the mode control and the output beam quality. The experiments described in succeeding paragraphs were performed to determine the beam degradation caused by this tip obscuration. Also, measurements were made of the radiation flux in the region of the W-axicon tip with and without an obscuration aperture using a new thermocouple technique.

The obscuration of the W-axicon tip was first accomplished by suspending a small steel ball in front of the tip with a fine wire. The use of a circular aperture in front of the W-axicon was more convenient, and there was concurrence between the two methods. The W-axicon transforms the optic axis of the compacted leg into a cylinder of 18.415 cm (7.25 in.) diameter in the annular leg. Circular apertures of 18.415 cm (7.25 in.), 18.315 cm (7.21 in.), 18.215 cm (7.17 in.), 17.915 cm (7.050 in.), and 17.415 cm (6.85 in.) diameter were used for these tests to provide equivalent obscuration diameters of 0, 1, 2, 5, and 10 mm.

The beam quality degradation was negligible for obscuration diameters of up to 2 mm for all the HSURIA resonators tested, namely, B, C, D, and E. For a 5-mm-diameter obscuration, however, the beam degradation was significant for resonators B, C, and D. The larger obscurations were not used with resonator E. Beam quality curves for resonator B are shown in Fig. 12 for no obscuration and for a 5-mm-diameter obscuration. The beam quality index, n^2, increases from 1.29 to 1.69 with the obscuration. The beam quality degradation for HSURIA configurations B, C, and D are shown in Fig. 13 as a function of obscuration diameter. These curves are all very similar, although the compacted leg lengths for C and D are twice that of resonator B. Mode control of a

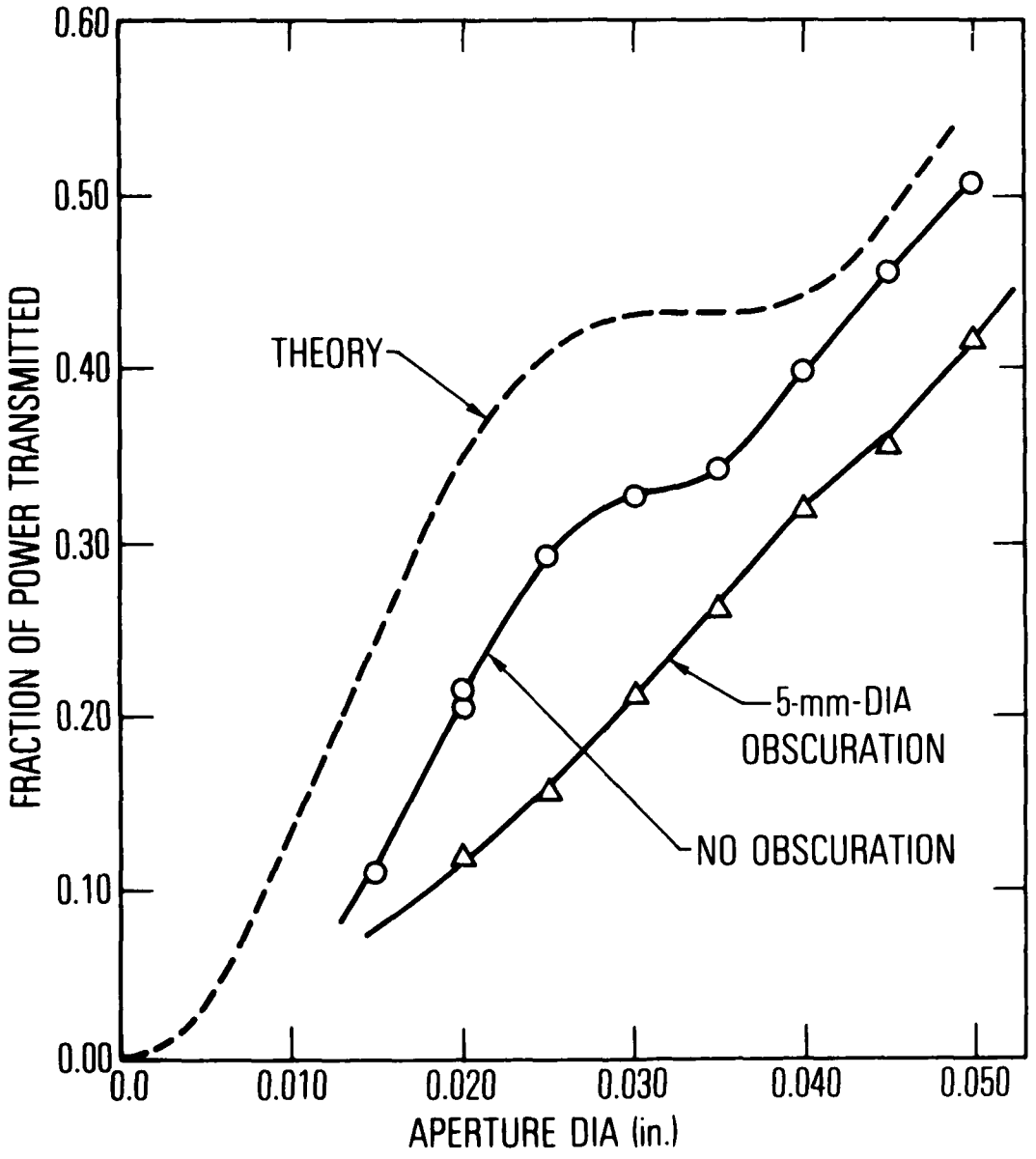

Fig. 12. Beam Quality Curves with and without W-Axicon Tip Obscuration

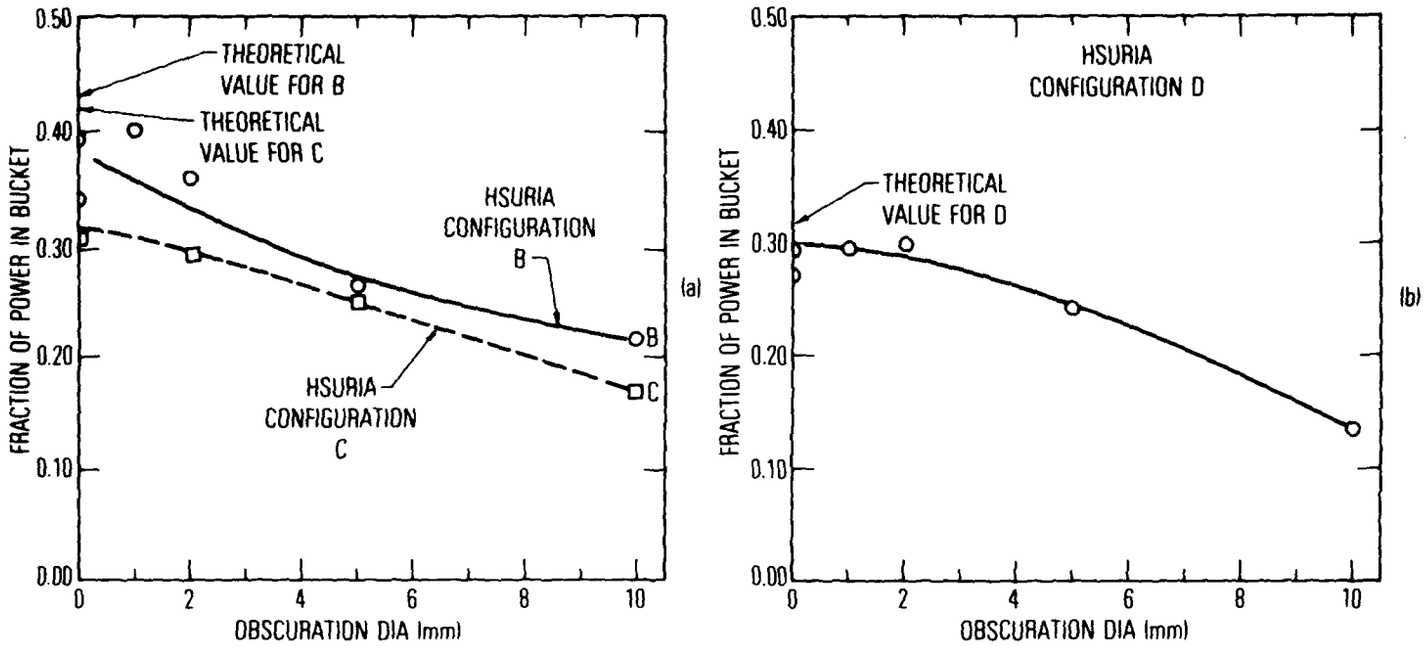

Fig. 13. Fraction of Power in Central Lobe vs Obscuration Diameter for Three HSURIA Configurations

HSURIA theoretically occurs in a central diffraction-limited core in the compacted leg. The simplest analysis of the preceding results is a comparison of the obscuration diameter with the size of this central core. Assuming the size of this core is determined by a Fresnel number of unity, then the diameter is

$$d = 2\sqrt{\lambda L_C}$$

For resonator B, with L_C = 1.31 m, d = 7.46 mm. For resonator C, where L_C = 2.66 m, d = 10.62 mm, and resonator D is approximately the same. A tip obscuration diameter of 2 mm is only one-fourth the size of the central core, and the effect on mode control is negligible. Significant beam degradation is observed when the obscuration diameter becomes comparable with the diameter of the diffraction-limited core.

VI. THERMOCOUPLE SCANS OF THE W-AXICON TIP REGION

For the initial test of tip obscuration, a small steel ball was suspended in front of the W-axicon tip with a thin nylon filament that was burned when the laser was turned on. It was then realized that there was a region of high flux near the tip, and a small thermocouple probe of 0.5 mm diameter was made from iron and constantan wire of 0.15 mm diameter to obtain measurements of this flux density. An approximate calibration of this thermocouple probe was obtained by placing it at the position of the thermal image screen where there is a magnified image of the far-field pattern. The relative radiant flux density at this location was determined by scanning the far-field pattern with a small aperture and an infrared detector. This scan is shown in Fig. 14. The total average power in the pattern was measured with a laser power meter to be 4.4 W. Approximately 33% of this power is in the central lobe that was determined to be 0.15 in. or 0.38 cm diameter from the detector scan. From these data it was estimated that the peak average flux density was about 4 W/cm^2. This produced an average temperature of 140°C. Furthermore, a comparison of the detector and thermocouple scans shows the latter response to be nearly linear.

Several vertical thermocouple scans at increasing distances from the W-axicon tip are shown in Fig. 15(a). The high-flux region has a half-width of 2 mm diameter and decreases to half its peak value at 2.5 mm from the tip. This high-field region is evidently caused by diffraction in the region of the cylindrical optic axis that is reflected radially inward by the outer cone and is not intercepted by the inner cone. The thermocouple junction intercepts a portion of this radiation, which is incident primarily from the radial direction, although a small fraction may come from the W-axicon tip. This latter contribution should not decrease as the thermocouple is moved from the tip. The peak flux density incident on the thermocouple junction can be estimated from the calibration with the far-field pattern. For the calibration, an average temperature of 140°C was obtained from an average flux density of 4 W/cm^2 incident from one side. A comparable average temperature was obtained

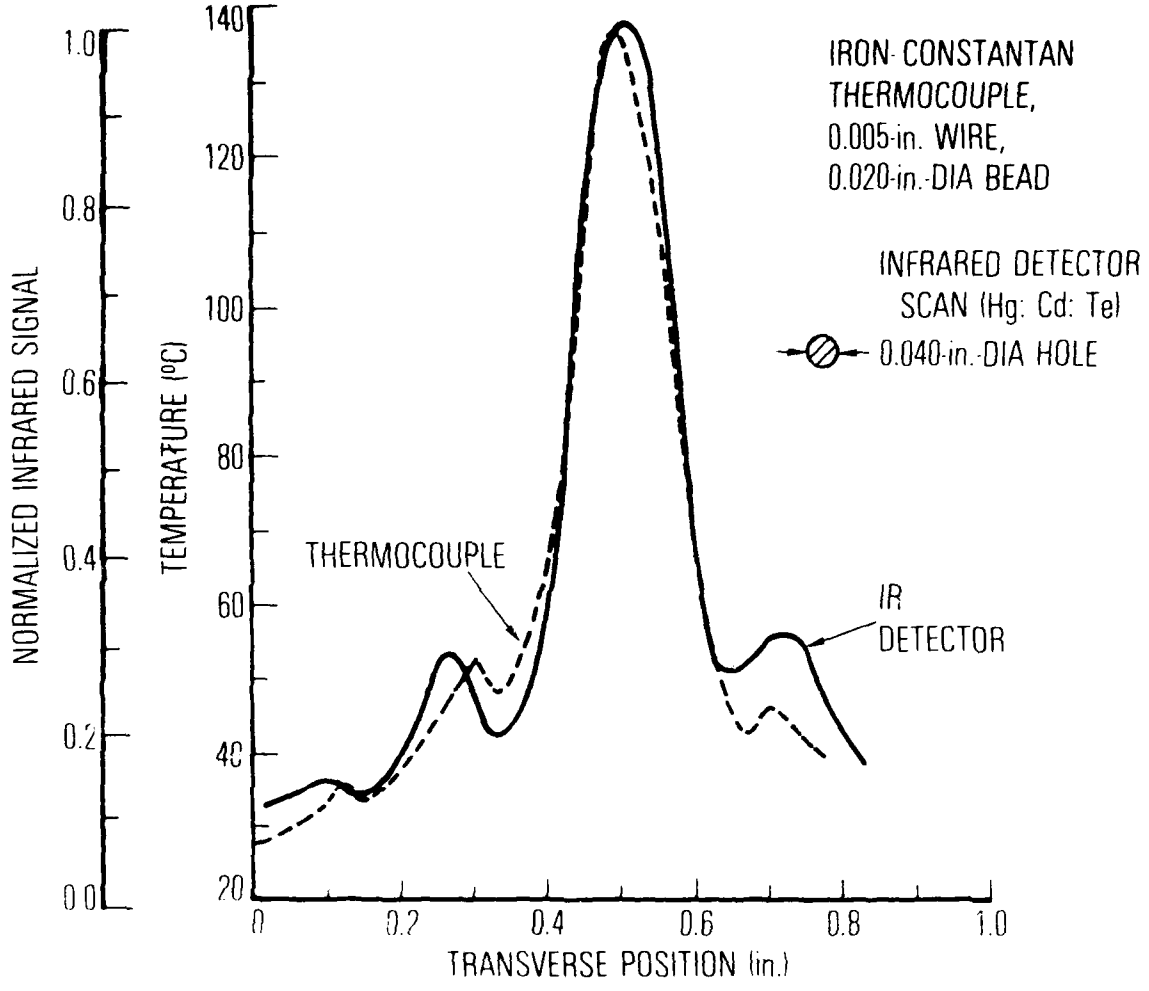

Fig. 14. Thermocouple and Detector Scans of Far-Field Intensity

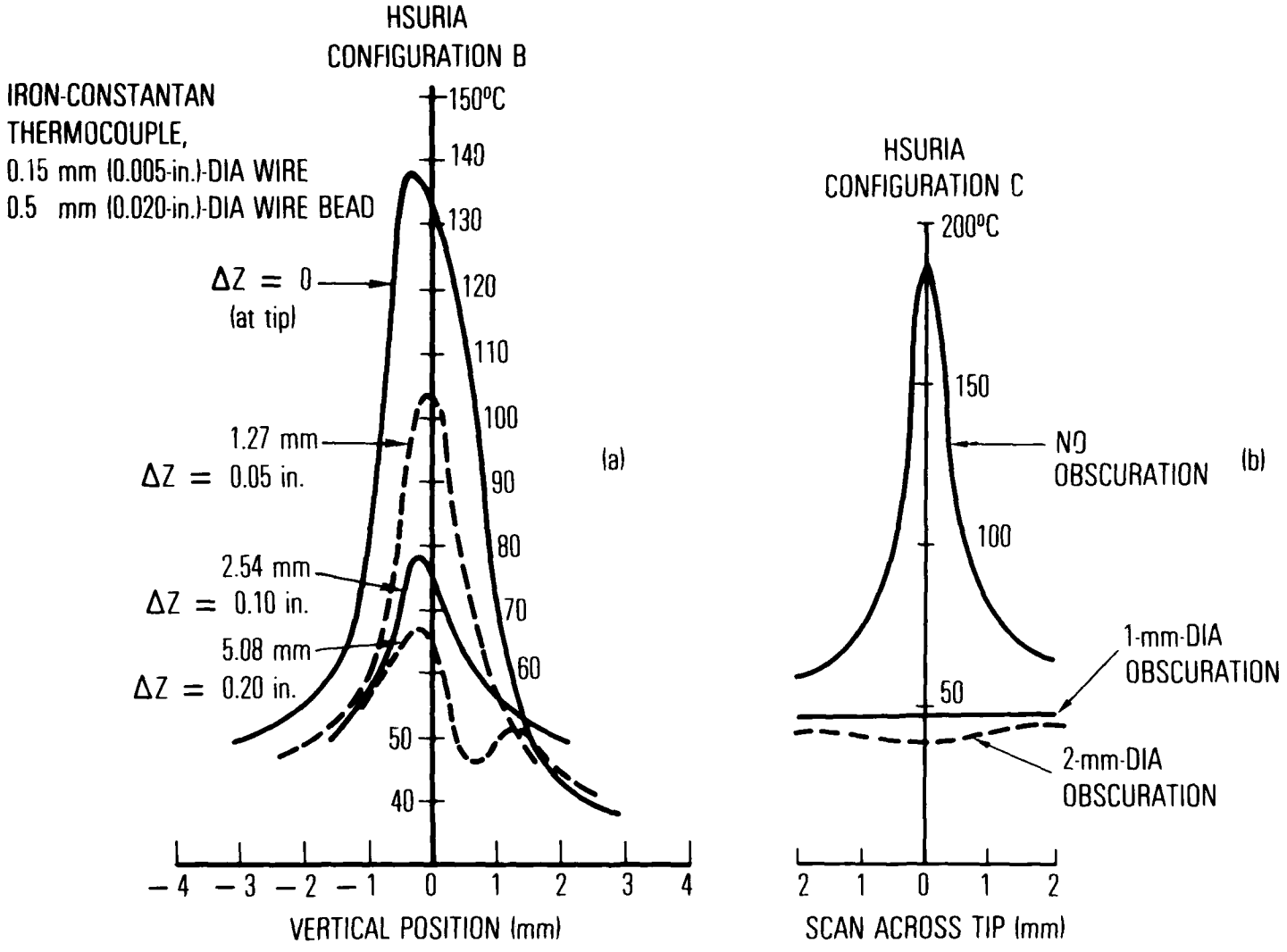

Fig. 15. Thermocouple Scans of Radiation Field Near W-Axicon Tip

near the W-axicon tip from radiation incident inward from the radial direction. From geometrical considerations, this average flux was approximately 1.0 W/cm^2. For a duty cycle of 1%, the peak flux during a pulse is nearly 100 W/cm^2. The apertures, which are slightly smaller in diameter than the optic axis, intercept this diffracted radiation, so the high-field region outside the tip disappears, as shown in Fig. 15(b).

Note that the flux incident on the W-axicon tip itself was not measured by these thermocouple scans, but this could be easily performed by scanning the thermocouple a short distance from the surface of the inner cone near the tip.

VII. POLARIZATION OF LASER OUTPUT BEAM

One should expect that the output beam of the HSURIA resonator with a W-axicon and flat rear cavity mirror should be linearly polarized,[2] and indeed the $\ell = 0$ mode that is observed is compatible with a linearly polarized output. There is, however, no optical element in the resonator cavity that would cause a preference for a given direction of the linear polarization. Observations of the direction of polarization of the laser output beam showed rapid fluctuations in the direction. Figure 16, for example, shows detector signals corresponding to the horizontal and vertical directions of polarization. The output is observed to switch rapidly in mid-pulse from a mostly vertical direction to a mostly horizontal direction.

An experiment was therefore designed to control the direction of polarization of the HSURIA with reflection polarizers that were described by Cox and Hass.[8] An optical diagram of this resonator is shown in Fig. 17. The two plane reflection polarizers were mounted between the convex mirror and the output coupling mirror (scraper). The output beam was then determined to be vertically polarized with a horizontal component of less than 2%, and the best beam quality observed was $n^2 = 1.3$, almost as good as that observed for the similar resonator configuration B. It is therefore possible to easily control the direction of linear polarization for a HSURIA resonator with a flat rear mirror using flat polarizing reflectors.

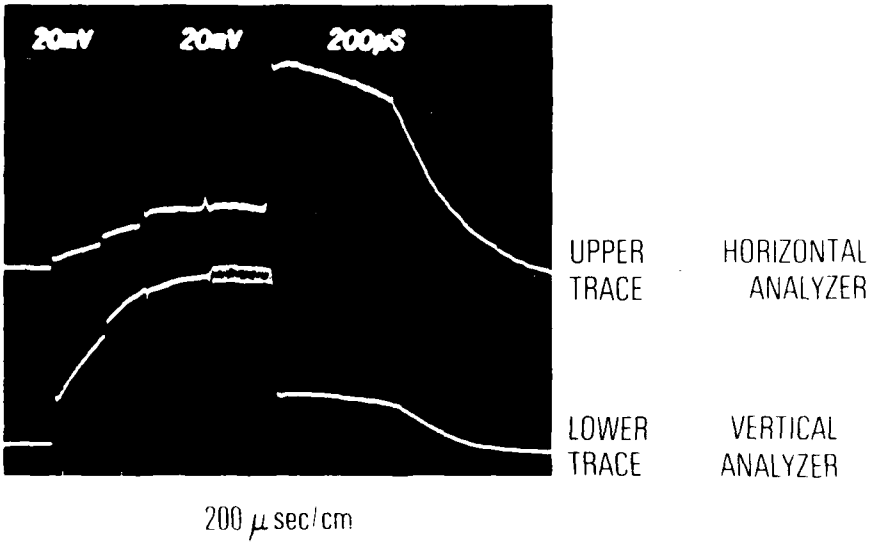

Fig. 16. Detector Signals Corresponding to Laser Output in Horizontal and Vertical Directions of Polarization

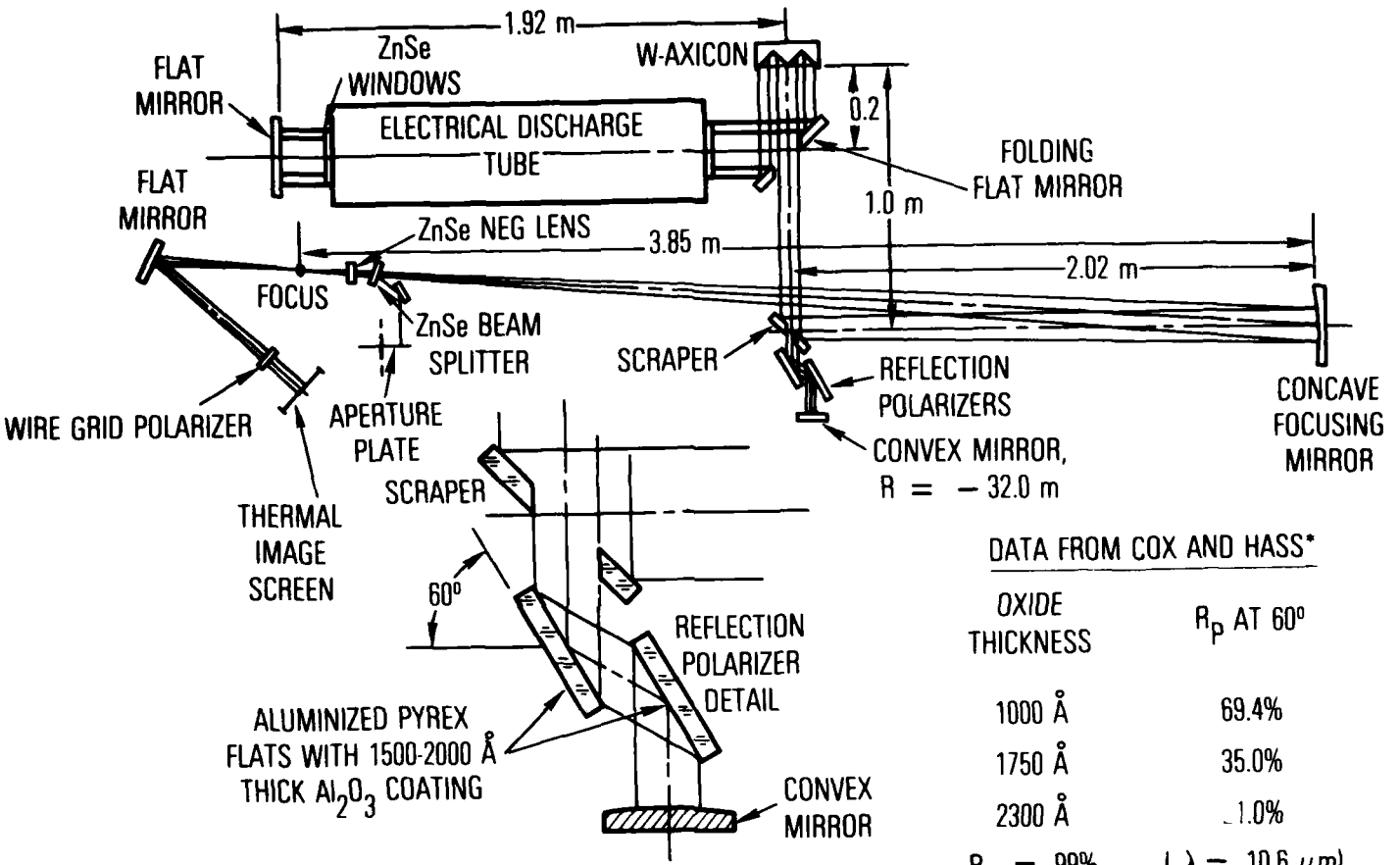

DATA FROM COX AND HASS*

OXIDE THICKNESS	R_p AT 60°
1000 Å	69.4%
1750 Å	35.0%
2300 Å	1.0%

R_S = 99% (λ = 10.6 μm)

*APPLIED OPTICS 17, 1657 (1978)

Fig. 17. Optical Diagram of Resonator with Reflection Polarizers

VIII. SUMMARY AND COMMENTS

The HSURIA with a W-axicon and a flat rear cavity mirror is capable of producing an $\ell = 0$ mode with a beam quality of better than $n^2 = 1.3$. This was considered adequate for experimental tests of several important effects associated with the use of this annular resonator with a real cylindrical chemical laser. First of all, the vibration caused by the operation of a chemical laser could result in misalignment of the optical elements. Measurements showed that even small misalignments of the rear flat mirror resulted in a severe degradation of beam quality, so a HSURIA with a rear flat mirror could not be used in a vibrational environment without the use of a sophisticated active control system. The spherical convex feedback mirror, however, was not sensitive to misalignment.

Secondly, struts must be used to provide support for the chemical laser gain generator inside the optical cavity and they must also be used to route gas feed lines to the gain generator. Our experiments have shown, however, that power losses of up to 30% (for six 5-deg struts) result when strut masks are placed in the annular beam of a HSURIA resonator. Analysis has shown that these losses result in part from diffraction effects and in part from the relatively low degree of saturation of the gain medium. Computer calculations taking both of these effects into account agree with our experimental power loss data.[7] For annular chemical lasers operating at shorter wavelengths and with higher gain, the power loss caused by struts would be closer to the geometric fraction of obscuration. Struts also produced a degradation of beam quality that increases with strut width.

It has been proposed that excessive heating of the W-axicon or reflaxicon tip, caused by the concentration of radiation at this point, can be reduced by a partial obscuration of the tip with an aperture. Our tests have shown that this can indeed be done without a significant degradation of beam quality as long as the effective or output power diameter of the obscuration is much smaller than a Fresnel zone, referred to the length of the compacted leg. An obscuration that is comparable in diameter to the Fresnel zone causes a loss

of mode control. While investigating the effects of tip obscuration, it was discovered that there is a region of high flux just outside the tip of the W-axicon, and this region was measured with a small thermocouple probe. This is reflected from the outer cone past the W-axicon tip, and it disappears when a circular aperture slightly smaller in diameter than the expanded optical axis is placed in front of the W-axicon. Finally, it has been demonstrated that the polarization of a HSURIA with a flat rear mirror can be controlled with a reflection polarizer without a degradation of beam quality.

APPENDIX

EFFECT OF DIFFRACTION AND GAIN SATURATION ON POWER LOSS CAUSED BY STRUTS

A. DIFFRACTION EFFECTS

A numerical model of the struts was developed in an effort to understand the cause of the large strut losses. Photographs of the near field show a pattern of light and dark bands in the vicinity of each strut, and the pattern does not meet between struts. Therefore, the numerical model chosen was Cartesian; i.e., it modeled only propagation past a single strut many times. Gain medium effects were neglected. In this analysis, a configuration was used where the struts are equidistant between the resonator mirrors such that the struts are the same distance, L, apart. The number of passes through consecutive struts was assumed to be ten. This corresponds to five roundtrips through the resonator, which is typical for the unstable cavities considered. A conventional iterative Fresnel-Kirchoff diffraction formulation was used to calculate the intensity distribution and integrated power at the strut location from one to ten passes. The calculation assumed L = 3.45 m (HSURIA cavity length), λ = 10.6 μ, and a strut half width ε = 2.01 mm (2-1/2-deg strut). The parameter used in the Fresnel diffraction calculation was $E = \varepsilon/\sqrt{\lambda L/2} = 0.42$, which is the normalized geometric half width of the strut. As the beam propagated between the struts, the effective half width gradually increased because of diffraction.

Figure A-1 shows the calculated intensity distribution at the strut location for the first and tenth passes. The corresponding integrated power or the "effective" half width is shown in Table A-1. It is apparent that there is significant widening of the strut image while going from one to ten passes. For the first and tenth passes, the first maxima occur at 3.5 and 10 times the geometric strut width, respectively. On the other hand, the power loss for the first and tenth passes is 1 and 2.5 times the geometric loss,

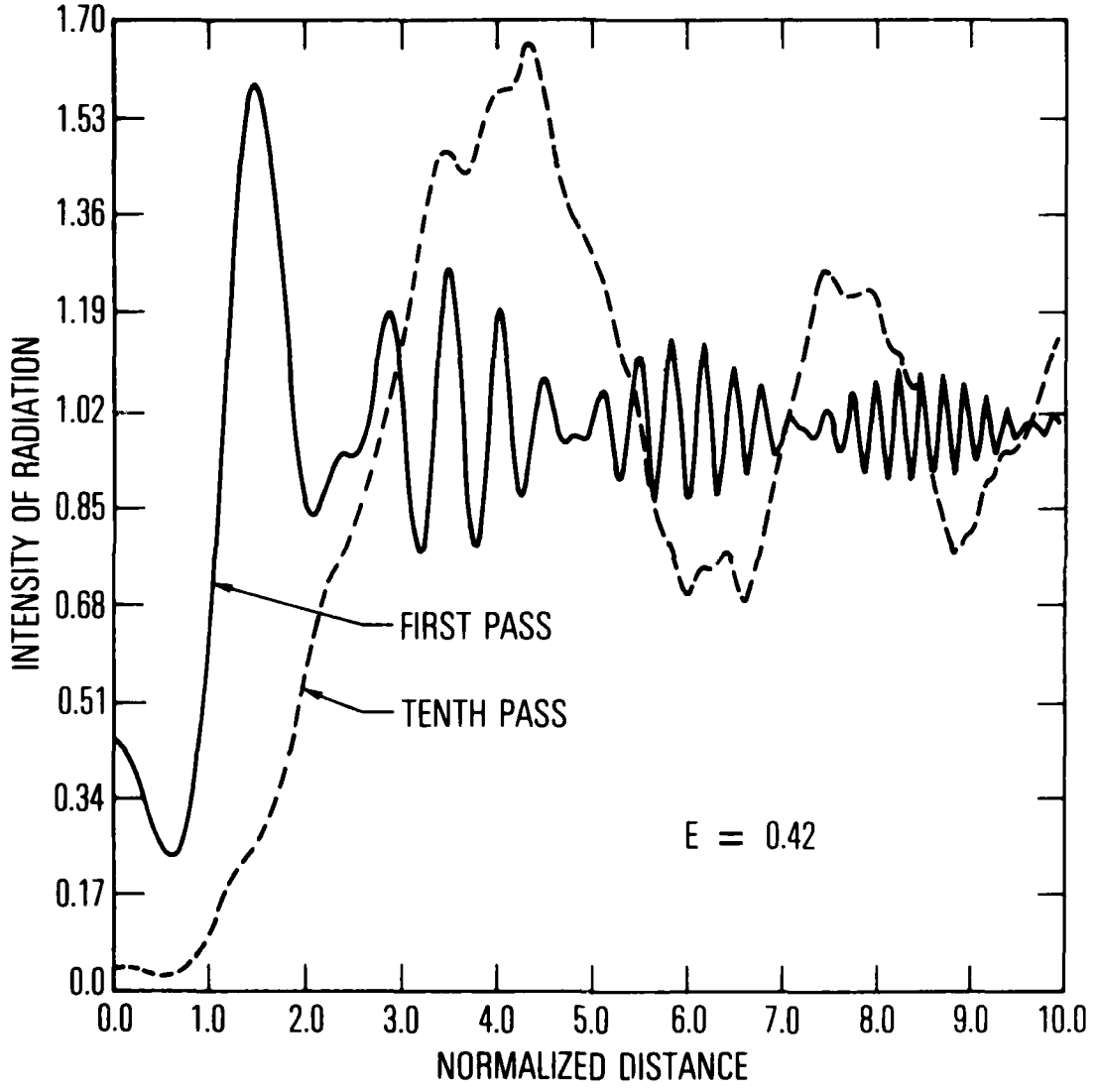

Fig. A-1. Diffraction Pattern Caused by Struts

Table A-1. Effective Strut Half-Width (E)

Pass No.	E
0	0.420
1	0.424
2	0.627
3	0.738
4	0.804
5	0.85
6	0.91
7	0.98
8	0.99
9	1.03
10	1.04

respectively. Thus, even though the strut image is much wider than the geometric strut, diffraction redistributes the intensity so that the power loss is reduced. The calculated power loss after ten passes for 2-1/2-deg struts is 2.5 times the geometric loss. Conversely, the measured power loss is six times the geometric loss for 2-1/2-deg struts. The difference is attributed to lack of gain saturation on our CO_2 test bed.

We have considered the effect of diffraction alone on the intensity distribution and power loss caused by struts. Another limiting case of interest is to neglect the effect of diffraction and consider only gain saturation effects. The numbers obtained from either limiting case, of course, will not be quantitative and will only be useful in showing trends. Conversely, a more complex analysis in which both diffraction within a resonator and gain saturation are simultaneously considered does not as readily pinpoint the important physical phenomena.

B. GAIN SATURATION EFFECTS

The strut blockage in the annular leg of a HSURIA can be considered an effective reflection loss that will increase the threshold gain and thereby reduce the power extraction. When a resonator is operating near threshold, a small reduction in reflectivity will produce a large decrease in output power, while if it is well above threshold, the output power variation will be reduced. From Rigrod's analysis it can be shown (within the homogeneous broadening approximation) that the output power from an unstable resonator, assuming a geometric loss is given by

$$\frac{P_{os}}{P_m} = \frac{P_{os}}{AI_o g_o \ell} = \left(1 - \frac{g_t}{g_o}\right)\left(1 - \frac{1}{M^2}\right)\Big/\left(1 - \frac{rr_s}{M^2}\right)$$

where

P_m = maximum power available from the gain medium = $AI_o g_o \ell$

I_o = saturation intensity $\simeq$ 4 W/cm^2

g_o = zero power gain $\simeq 1.25\ m^{-1}$

ℓ = gain length = 0.92 m

A = area of mode in gain region

g_t = threshold gain

$= \frac{1}{\ell} \ln (M/\sqrt{r r_s})$

M = resonator magnification = 1.9

r = roundtrip reflectivity of mirrors $\simeq (0.98)^8 = 0.851$

r_s = effective roundtrip reflectivity due to struts = r_{1s}^2

($P_{os} \equiv P_o$ for the no-strut case where $r_s = 1.0$)

r_{1s} = single pass reflectivity due to struts

The observed fractional power loss caused by struts is given by $(1 - P_{os}/P_o)$. The ratio $P_o/P_m = 0.352$ shows that the laser is operating in an unsaturated regime. In order to produce a 25% loss in total output power, a single pass reflectivity caused by strut obscuration of $r_{1s} = 0.914$ is required. Thus, to produce the measured 25% power loss for six 2-1/2-deg struts at the position of the W-axicon, a single pass strut loss of 8.6% is indicated for gain saturation effects alone. This is more than twice the geometric strut loss of 4.2%, so diffraction effects are still important. For six 5-deg struts that produce a 30% power loss (Table 3), a single pass strut loss of 10.4% is required which is close to the geometric value of 8.4%. Thus, it appears that for 5-deg struts, diffraction effects are less important, and the losses are nearly geometric.

Next consider the case of the struts located near the flat mirror in the HSURIA annular leg. For this case the radiation field hits the struts only once per roundtrip, and r_s corresponds to the single pass strut reflectivity. Experimentally, 14 and 20% power losses were measured for six 2-1/2- and six 5-deg struts, respectively. Single pass strut losses of 9.4 and 13.3% are calculated for the 2-1.2- and 5-deg struts, respectively. This is near the

calculated single pass strut losses for the case of the struts located near the W-axicon. The losses are slightly larger because the strut mask was located a small distance from the flat mirror near the window of the gain cell.

Finally, with the aid of the simple homogeneous gain model, we can investigate the effectiveness of reducing the magnification of the unstable resonator to increase the saturation of the gain medium versus increasing the gain length. By reducing the magnification from 1.9 to 1.4 and keeping all the other parameters the same, the single pass strut loss to produce a 25% power loss is 9.9%, nearly the same as the M = 1.9 case. Alternatively, changing M = 1.9 to 1.4 for the same single pass strut loss of 8.6% would only reduce the output power loss from 25 to 22%. Thus, decreasing the magnification from 1.9 to 1.4 would not have a significant effect on the output power loss for the six 2-1/2-deg struts. This is consistent with our experimental results, whereas, the output power loss caused by struts was essentially the same for the M = 1.9 resonator compared with an M = 1.5 resonator.

If one increases the gain length from ℓ = 0.92 m to ℓ = 1.5 m, and leaves the other parameters the same (M = 1.9), a 25% power reduction corresponds to a 17.3% single pass strut loss or an 8.6% strut loss (ℓ = 0.92 m, 2-1/2-deg strut case) corresponds to a 13% output power reduction. Thus, increasing the gain length to ℓ = 1.5 m should significantly reduce the observed output power losses caused by struts, and data more representative of a saturated high power device would be obtained. The penalty would be an increased cavity length and a reduction in the range of equivalent Fresnel numbers that could be studied.

REFERENCES

1. E. B. Turner and R. A. Chodzko, "Large Diameter CO_2 Laser Facility for Testing Optical Resonators," manuscript submitted for publication.

2. R. A. Chodzko, S. B. Mason, E. B. Turner, and W. W. Plummer, Jr., "Annular (HSURIA) Resonators: Some Experimental Studies Including Polarization Effects," Appl. Opt. 19, 778 (1980).

3. T. C. Salvi, "Correction to Equivalent Fresnel Number . . . . .," unpublished Air Force Weapons Laboratory technical memorandum.

4. Born and Wolfe, "Principles of Optics," Second (Revised) Edition, p. 416.

5. W. F. Krupke and W. R. Sooy, "Properties of an Unstable Confocal Resonator CO_2 Laser System," QE-5, 575 (1969).

6. I. A. Abramowitz, Hughes Aircraft, Culver City, Calif., private communication.

7. A. Seminov, Rocketdyne Division of Rockwell International, Canoga Park, Calif., private communication.

8. J. T. Cox and G. Hass, "Highly Efficient Reflection-Type Polarizers for 10.6 λm CO_2 Laser Radiation . . . . .," Appl. Opt. 17, 1657 (1978).

LABORATORY OPERATIONS

The Laboratory Operations of The Aerospace Corporation is conducting experimental and theoretical investigations necessary for the evaluation and application of scientific advances to new military space systems. Versatility and flexibility have been developed to a high degree by the laboratory personnel in dealing with the many problems encountered in the nation's rapidly developing space systems. Expertise in the latest scientific developments is vital to the accomplishment of tasks related to these problems. The laboratories that contribute to this research are:

Aerophysics Laboratory: Launch vehicle and reentry aerodynamics and heat transfer, propulsion chemistry and fluid mechanics, structural mechanics, flight dynamics; high-temperature thermomechanics, gas kinetics and radiation; research in environmental chemistry and contamination; cw and pulsed chemical laser development including chemical kinetics, spectroscopy, optical resonators and beam pointing, atmospheric propagation, laser effects and countermeasures.

Chemistry and Physics Laboratory: Atmospheric chemical reactions, atmospheric optics, light scattering, state-specific chemical reactions and radiation transport in rocket plumes, applied laser spectroscopy, laser chemistry, battery electrochemistry, space vacuum and radiation effects on materials, lubrication and surface phenomena, thermionic emission, photosensitive materials and detectors, atomic frequency standards, and bioenvironmental research and monitoring.

Electronics Research Laboratory: Microelectronics, GaAs low-noise and power devices, semiconductor lasers, electromagnetic and optical propagation phenomena, quantum electronics, laser communications, lidar, and electro-optics; communication sciences, applied electronics, semiconductor crystal and device physics, radiometric imaging; millimeter-wave and microwave technology.

Information Sciences Research Office: Program verification, program translation, performance-sensitive system design, distributed architectures for spaceborne computers, fault-tolerant computer systems, artificial intelligence, and microelectronics applications.

Materials Sciences Laboratory: Development of new materials: metal matrix composites, polymers, and new forms of carbon; component failure analysis and reliability; fracture mechanics and stress corrosion; evaluation of materials in space environment; materials performance in space transportation systems; analysis of systems vulnerability and survivability in enemy-induced environments.

Space Sciences Laboratory: Atmospheric and ionospheric physics, radiation from the atmosphere, density and composition of the upper atmosphere, aurorae and airglow; magnetospheric physics, cosmic rays, generation and propagation of plasma waves in the magnetosphere; solar physics, infrared astronomy; the effects of nuclear explosions, magnetic storms, and solar activity on the earth's atmosphere, ionosphere, and magnetosphere; the effects of optical, electromagnetic, and particulate radiations in space on space systems.

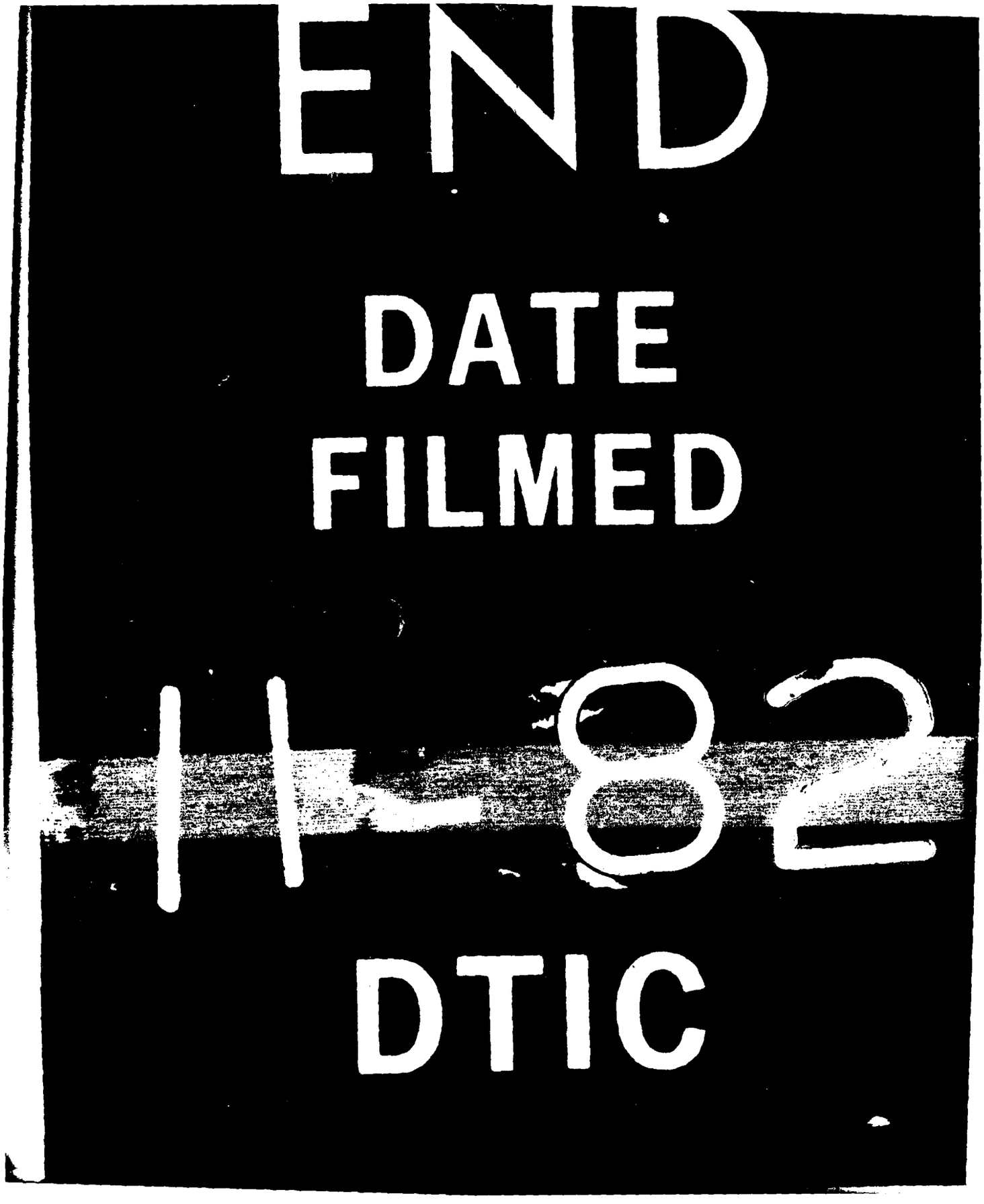
END
DATE
FILMED
11-82
DTIC